3 2 5
3 4/63

IDO-14601
December 1962

PHASE TRANSFORMATIONS IN CALCINATION OF NITRATES OF ALUMINUM, STAINLESS STEEL, AND NICHROME

Al,

MASTER

H. J. Eding, M. L. Huggins, A. G. Brown
(Stanford Research Institute)

PHILLIPS
PETROLEUM
COMPANY

PHILLIPS
66

ATOMIC ENERGY DIVISION

NATIONAL REACTOR TESTING STATION
US ATOMIC ENERGY COMMISSION

PRICE $1.50

Available from the
Office of Technical Services
U. S. Department of Commerce
Washington 25, D. C.

Printed in USA

IDO-14601
AEC Research & Development Report
Waste Disposal and Processing
TID-4500 (18th Ed.)
Issued: December 28, 1962

PHASE TRANSFORMATIONS IN CALCINATION OF NITRATES OF ALUMINUM, STAINLESS STEEL, AND NICHROME

H. J. Eding, M. L. Huggins, A. G. Brown
(Stanford Research Institute)

PHILLIPS
PETROLEUM
COMPANY

Atomic Energy Division
Contract AT(10-1)-205
Idaho Operations Office
U. S. ATOMIC ENERGY COMMISSION

FOREWORD

Highly radioactive liquid waste is produced at the Idaho Chemical Processing Plant (ICPP) during the recovery of spent aluminum-uranium test reactor fuels for the Atomic Energy Commission. A process has been developed and a demonstration plant built at the ICPP for the conversion of the liquid waste to a free-flowing solid for improved storage characteristics.

In addition to process studies on calcination at the ICPP, Phillips Petroleum Company in 1961 subcontracted a basic chemical investigation on the phase transformations in alumina to the Stanford Research Institute. The contract was granted in two parts; the results of the first part were published February 1962 as IDO-14580 by H. J. Eding, M. L. Huggins, and A. G. Brown. The second part of the contract is published herewith and completes the program, at least as far as it can be taken at this time.

The second part of the study is devoted to an application of the use of boric acid to the 60-gallon-per-hour Demonstration Waste Calciner Facility (DWCF), and to transformation studies in the calcination of waste solutions containing nitrates of iron, chromium, and nickel. Small concentrations of agents, such as 0.01$\underline{M}$ molar boric acid, when added to the calciner feed, have produced a surprisingly improved performance of the fluid bed by reducing the overhead fines and making those solids readily soluble for recycle that did go overhead. The boric acid keeps the alumina in the amorphous rather than crystalline state. The presence of non-radioactive fission products in laboratory calcination experiments had no unusual effects on the operation. The DWCF has been put through an intensive test program with non-radioactive material, and a flowsheet successfully demonstrated. The final test was a 30-day continuous run in which 400 curies of sodium-24 in two additions of 50 and 350 curies were used as tracer; the bed and product remained amorphous in alumina (below 0.5 per cent in alpha alumina) and the process was operable.

The work on stainless steel-containing wastes was done with a view toward extending fluid bed calcination to wastes from the Electrolytic or Darex processes. However, considerable work remains before a meaningful full-level run will be made in the DWCF on aluminum wastes. Until then, the work on other wastes must remain of a preliminary nature.

The development studies by R. F. Murray and D. W. Rhodes on aluminum calcination have been fully reported in IDO-14581. This work was complementary to the Stanford program. Related studies on stainless steel at the ICPP by E. M. Vander Wall are reported in IDO-14597, "Thermal Decomposition of Hydrated Iron, Chromium, and Nickel Nitrates and their Mixtures." The data in IDO-14597 were referred to in the current report in references 2 and 7. On page 39 the chromium compound formed at 260-390°C has since been found to be amorphous and have the empirical formula $CrO_{2.2}$.

Samples of calcined product from runs F-9 through 14 from page 12 of the SRI study were sent to the ICPP for analysis and characterization. The results were not available in time for incorporation in the terminal report, but are reported in the following tables. The attrition index is the weight per cent of solids remaining unchanged in size after being fluidized in a column for 30 minutes. A 25 gram sample is used from the size range -20+35 mesh. The control sample was an amorphous product from the ICPP pilot plant.

PARTICLE PROPERTIES OF CALCINED STAINLESS STEEL OXIDES

Particle Properties and Nitrate Content

Run No.	Bulk Density (g/cc)	Absolute Density (g/cc)	Particle Density (g/cc)	Intra-Particle Porosity (fraction)	Mass Median Particle Diameter (mm)	Nitrate Content (m-moles/g)
F-9	1.06	2.61	1.59	0.39	0.82	1.11
F-10	2.04	4.85	3.44	0.29	0.57	< 0.12
F-11	1.99	5.07	2.92	0.43	0.66	< 0.12
F-12	1.73	4.68	2.56	0.45	0.66	< 0.12
F-13	1.78	5.79	3.13	0.46	0.45	< 0.1
F-14	1.33	5.11	2.61	0.49	0.42	< 0.12

ATTRITION INDEX FOR CALCINED METAL OXIDES

Sample	Attrition Index
Control Alumina - ICPP Calcined	85.4
F-9 Alumina - SRI Calcined	93.8
F-10 Iron oxide	75.2
F-11 SS oxides	80.1
F-12 SS oxides +B	81.5
F-13 Nickel oxide	(insufficient sample)
F-14 Nickel oxide +B	13.8

C. M. Slansky
Technical Liaison Representative
Atomic Energy Division
Phillips Petroleum Company

IDO-14601 is reprinted without change from SRI Project No. PU-3662, same title, issued October 10, 1962, by Stanford Research Institute of Menlo Park, California.

STANFORD RESEARCH INSTITUTE
MENLO PARK, CALIFORNIA

October 10, 1962

Final Report | *January to October, 1962*

PHASE TRANSFORMATIONS IN CALCINATION OF NITRATES OF ALUMINUM, STAINLESS STEEL, AND NICHROME

Prepared for:

ATOMIC ENERGY DIVISION
PHILLIPS PETROLEUM COMPANY
IDAHO FALLS, IDAHO

PROJECT AGREEMENT NO. 28 UNDER
CONTRACT AT-(04-3)-115

By: H. J. Eding, M. L. Huggins, A. G. Brown

SRI Project No. PU-3662

Approved:

A. E. GORUM, DIRECTOR
MATERIAL SCIENCES DIVISION

Copy No............

PHASE TRANSFORMATIONS IN CALCINATION OF NITRATE SOLUTIONS OF ALUMINUM, STAINLESS STEEL, AND NICHROME

H. J. Eding
M. L. Huggins
A. G. Brown

ABSTRACT

Earlier studies (IDO-14580) had shown that low concentrations of boric acid would inhibit the formation of alpha alumina in the fluidized calcination of aluminum nitrate wastes. Studies designed to determine the optimum concentration of boric acid and the relative effectiveness of phosphoric acid were performed by heating synthetic mixtures at moderate pressure, and showed that they were equally effective at the same molal concentration. Differential thermal analysis of mixtures showed that the boric acid reacted with alumina below 183°C. Extraction of boric acid from selected samples indicated that the boron was bonded (probably in a random manner, as in glasses) to the alumina rather than to sodium. Addition of fission products was studied, and no unusual effects were found.

The transformation studies on calcination of stainless steel nitrates indicated that alpha iron oxide would be formed even with the addition of moderate amounts of additives such as boric acid, phosphoric acid, or aluminum nitrate, or combinations. Rare earths were the most effective additive. Similar studies on nichrome wastes indicated that nickel oxide (crystalline) would be formed even with additives. The studies included heating of synthetic mixtures at moderate pressure, differential thermal analysis, and use of a laboratory fluidized calciner.

CONTENTS

CONTENTS (Concluded)

FIGURES

TABLES

I INTRODUCTION

High-level radioactive liquid wastes are produced in the processing of uranium reactor fuel elements. The solutions contain waste fission products and the inert components of the fuel. The main components of the solutions studied here consisted of nitric acid and nitrates from aluminum, stainless steel, or nichrome. The acidic wastes are currently stored in underground tanks, and processes are being developed to convert these solutions into stable solids. The fluid bed calcination of aluminum nitrate to free-flowing powdered alumina is being developed at the Idaho Chemical Processing Plant, using a 2-ft-square fluidizer in a pilot plant[1] and a Demonstration Waste Calcining Facility[2](DWCF). A change in product properties was observed which correlated with an increase in the alpha alumina content of the product.[1] The operations were satisfactory when the product was amorphous; but when the alpha alumina content increased, then the average particle size decreased, the off-gas loading increased, and the bulk density increased. The factors influencing the formation of alpha alumina needed to be known. The objective of the original contract was to conduct a basic investigation of the formation of various forms of alumina from aqueous solutions by calcination, including a study of the effects of temperature, irradiation, minor components and impurities, etc., upon the phase transformation and upon the equilibrium phase diagram. The results were published in a Technical Report,[3] IDO-14580, "Phase Transformations in Alumina," covering the period May to December 1961.

The report (IDO-14580) showed that synthetic aluminas (prepared in the laboratory and heated in a micro reactor at pressures above 150 psi) formed alpha alumina. The effect of impurities or additives seemed to correlate with the formation of alpha alumina in the pilot plant fluidizer. Boric acid, phosphoric acid, magnesium, and fission products (at ten times the expected amount) appeared to prevent the formation of alpha alumina. Other additives, such as sodium, calcium, iron, and lithium favored the formation of alpha alumina. Potassium, zinc, sulfate, and silicate had no effect. Tests using boric acid in the pilot plants at Idaho Falls showed very favorable results, but additional laboratory data were desired to determine optimum concentrations of boric acid and phosphoric acid.

Other studies reported[3] included new intermediate phases between aluminum nitrate and aluminum oxide, electron diffraction studies of the cross section of particles, differential thermal analysis of aluminum nitrate and alumina from the pilot plant, structure of amorphous alumina using the radial distribution method, a discussion of factors influencing the formation of alpha alumina, and a theoretical discussion of the effect of additives.

A recent report[4] by Murray and Rhodes also contains information on the effect of sodium and other factors which aid formation of the alpha alumina, and on the inhibiting effect of boric acid.

This report covers research on an extension of the original contract. The objective of this research was to establish optimum conditions for calcination of aluminum nitrate waste solutions by use of suitable additives that would prevent the formation of alpha alumina and an excessive amount of fines. Samples from pilot plant runs were to be examined by electron diffraction and other specialized instrumental techniques. Experiments were made to determine the reactions, effects, and phase transformations which occur with certain additives, such as boric acid. Similar studies to those for aluminum were to be done for the waste solutions from processing of stainless steel and nichrome.

II SUMMARY AND CONCLUSIONS

Transformation studies were made on synthetic aluminas prepared from aluminum nitrate with various additives. Several tests indicated that boric acid and phosphoric acid at equal mole ratios to alumina were equally effective for prevention of formation of alpha alumina. Tests on the effect of fission products indicated that the rare earths and molybdenum tended to prevent the formation of alpha alumina, while barium, cesium, and zirconium either had no effect on alpha formation or aided it. The studies with fission products at their expected concentrations indicated that they would not significantly affect the formation of alpha alumina nor interfere with the use of boric acid to control crystallinity. The minimum temperature for formation of alpha alumina at moderate pressure was found to be below 325°C.

Differential thermal analysis studies on the reaction of boric acid and sodium nitrate with amorphous alumina (Sample IVA) indicated a reaction with boric acid below 183°C and at least a partial reaction with sodium nitrate below 320°C.

Observations on the effect of additives on evaporation of aluminum nitrate solutions indicated that 0.6 mole of phosphoric acid per mole of alumina might be useful for pot calcination.

Transformation studies on samples from the pilot plant with varying amounts of boric acid indicated that the equilibrium phase diagram for alumina with sodium would have an α-Al_2O_3 region up to 0.06 mole of B_2O_3 per mole of Al_2O_3, and a 2-phase region containing α-Al_2O_3 and $9Al_2O_3 \cdot 2B_2O_3$ from 0.06 to 0.22 moles B_2O_3 per mole of Al_2O_3. However, the boron and aluminum atoms are randomly distributed in an amorphous structure which is difficult to crystallize, and 0.01 to 0.06 mole of boric acid per mole of alumina might adequately control the crystallization of alpha alumina.

Extraction studies to determine the nature of the bonding of boron in the alumina indicated that the boron bonded to alumina rather than to sodium, and therefore that boron prevents crystallization by forming a random distribution with aluminum atoms in a network of oxygen atoms.

Electron diffraction studies of a few pilot plant samples agreed with earlier results that alpha alumina forms uniformly in portions of particles. Microscopic studies gave a correlation with the sharpness of concentric layers with alpha alumina content.

X-ray and electron diffraction studies on the acid-insoluble fraction of samples of amorphous alumina gave alpha alumina as the only detected phase. The X-ray diffraction analysis for alpha alumina was low owing to residual amorphous alumina or inadequate correction for the difference in crystallite size between samples and standards.

Fluidization studies with a laboratory fluidizer gave a very good amorphous alumina with aluminum nitrate waste solutions. The operation with stainless steel nitrates was a little more difficult and the product contained α-Fe_2O_3. The addition of boric acid reduced crystallization, but the product from pilot plant operation is likely to be crystalline. The operation with nichrome wastes was very difficult and the product was nickel oxide, determined by X-ray analysis. The addition of boric acid did not change the operation.

Transformation studies on stainless steel wastes showed that α-Fe_2O_3 was formed in all cases, even with additions of boric acid, phosphoric acid, aluminum, and combinations of these. Similar results were found for nichrome wastes with nickel oxide being formed. Rare earths were the most effective additives for stainless steel wastes.

Differential thermal analysis studies on nitrates of stainless steel and nichrome showed that stainless steel formed oxides at a lower temperature than aluminum nitrate, whereas nichrome required a higher temperature. A mixture of nichrome and stainless steel wastes acted like stainless steel wastes.

III PHASE TRANSFORMATIONS IN CALCINATION OF ALUMINUM WASTES

A. Transformations in Alumina at Moderate Pressure

The optimum concentrations of boric acid and phosphoric acid to control the formation of alpha alumina were to be determined by heating synthetic oxides in a micro reactor at pressures above 150 psi. Other tests were made to determine the effects of fission products on formation of alpha alumina and the minimum temperature for forming alpha alumina.

Synthetic aluminas were prepared for these tests from solutions of aluminum nitrate plus various additives. The compositions of the solutions are given in Appendix A. These solutions were evaporated nearly to dryness in Pyrex beakers on a hot plate and then heated in a muffle furnace for 16 hours at temperatures of 200 or 300°C. This method of preparing the synthetic aluminas is referred to as the boil-down method. The synthetic aluminas were ground to -100 mesh. The compositions of the synthetic aluminas are given in Appendix B. Two samples from the original project[3] were prepared by the drip method, in which the solution was allowed to drip into a heated stainless steel beaker.

These synthetic aluminas were placed in Pyrex containers and heated in an Aminco micro reactor at temperatures to 430°C and pressures to 370 psi and periods of time to a week. Usually five samples were run at a time, and Sample IV A from the pilot plant was included as a control. The pressure was built up from dehydration and decomposition of the nitrates and excess pressure was released for many of the runs. The results are given in Appendix C and are summarized in Table I. Samples EP, DD, and DI contained sodium and formed some alpha alumina, sodium nitrate, and A-phase. (Note: A-phase is the same as Form KI reported by Torkar[5]). These results agreed with the results reported earlier.

Samples CD-CG and CR, with an 0.06 mole ratio of sodium to aluminum and a boric oxide mole ratio from 0.02 to 0.46, did not form any alpha alumina. Aluminum borate, $9Al_2O_3 \cdot 2B_2O_3$, appeared at a B/Al mole ratio

Table I

ALUMINAS HEATED UNDER PRESSURE AT 430°C

Alumina[1]	Mole Ratios to Al_2O_3				X-Ray Data[3]
	Additive	Na_2O	H_2O	NO_3^-	
EP		.06	.31	.12	α(12%),NaN(19),A(15)
DD		.15	.44	.35	α(26%),NaN(75),A(8)
DI		.15	.33	.32	α(36%),NaN(47),γ(5)
DN	.22 B_2O_3	.00	.53	.03	-
CG	.02 B_2O_3	.06	.38	.09	γ(6),A(4),NaN(2)
CF	.05 B_2O_3	.06	.32	.07	γ(6),A(4),NaN(6)
CE	.09 B_2O_3	.06	.27	.05	γ(4),A(6),AlB(4),NaN(4)
CR	.34 B_2O_3	.08	.53	.28	AlD(90),NaN(52)
CD	.46 B_2O_3	.06	.25	.07	AlB(160),NaN(11)
DL	.007 B_2O_3	.15	.46	.31	α(1%),NaN(32),γ(5)
DJ	.013 B_2O_3	.15	.45	.27	α(4%),NaN(32),γ(4)
DB	.025 B O	.15	.54	.32	A(14),NaN(46),γ(3)
CZ	.05 B_2O_3	.15	.44	.29	A(4),NaN(27),γ(6)
CX	.10 B_2O_3	.15	.44	.28	A(9),NaN(50),γ(6)
CQ	.03 P_2O_5	.08	.58	.28	A(15),NaN(48),AlP(3)
CH	.05 P_2O_5	.06	.50	.09	A(4),NaN(5),γ(5)
CP	.12 P_2O_5	.08	.63	.26	A(8),NaN(45),AlP(22)
CO	.24 P_2O_5	.08	.52	.25	A(4),NaN)38),AlP(80)
CN	.60 P_2O_5	.08	.43	.27	NaN(40),AlP(230)
DM	.007 P_2O_5	.15	.54	.32	A(14),NaN(36),γ(3)
DK	.013 P_2O_5	.15	.48	.28	α(4%),NaN(27),γ(5)
DC	.025 P_2O_5	.15	1.07	.33	NaN(56),AlP(9),αH_2O(105)
DA	.05 P_2O_5	.15	.37	.28	A(11),NaN(25),AlP(4),γ(4)
CY	.10 P_2O_5	.15	.36	.21	A(6),NaN(33),γ(4)
CI	.02 B_2O_3+.02 P_2O_5	.06	.80	.29	α(1%),A(10),NaN(42)
CJ	.004 BaO+.009 Cs_2O	.06	.48	.23	α(25%),A(14),NaN(33)
CK	.012 MoO_3	.06	.46	.18	A(21),NaN(35)
CL	.014 ZrO_2	.06	.57	.22	α(5%),A(20),NaN(36)
CM	.003 Ce_2O_3+.004 La_2O_3	.06	.61	.24	A(32),NaN(31)
EO	.003 F.P.	.06	.18	.13	α(81%),NaN(18)
EQ	.003 F.P.+.006 B_2O_3	.06	.30	.13	α(17%),NaN(27),A(41)
EN	.005 F.P.	.06	.28	.13	α(38%),NaN(29),A(15)
ER	.005 F.P.+.006 B_2O_3	.06	.32	.17	NaN(11),A(15)
CW	.18 Fe_2O_3+.03 NiO +.035 Cr_2O_3	.06	-	-	α(6%),αH_2O(21),αFe_2O_3(8), NaN(7)

[1] See Appendixes A, B, and C for further details.

[2] Mole ratios to Al_2O_3 for fission products (F.P.) in samples EN and EO were RuO_2 0.0004, ZrO_2 0.0014, BaO 0.0004, Ce_2O_3 0.0003, La_2O_3 0.0004, MoO_3 0.0012, Cs_2O 0.0008. Samples EQ and ER had twice these concentrations.

[3] Alpha alumina contents are reported in percent. Other phases are followed by the intensity in arbitrary scale divisions (enclosed in parentheses). A = A phase, NaN = $NaNO_3$, AlP = $AlPO_4 \cdot 2H_2O$, AlB = $9Al_2O_3 \cdot 2B_2O_3$.

of 0.09. Samples DL, DJ, DB, CZ, and CX, with a higher amount of sodium, did form a small amount of alpha alumina with a boric oxide mole ratio of 0.013. The results indicated that boric oxide at very low concentrations is effective in preventing alpha alumina formation. However, it should be noted that samples from the pilot plant contained higher concentrations of alpha alumina than were formed in these experiments.

Samples CH, CN-CQ, CY, DA, DC, DK, and DM with phosphoric acid in place of boric acid gave similar results except that $AlPO_4 \cdot 2H_2O$ appeared at a B/Al mole ratio of 0.03. A comparison of the results at equal mole ratios of phosphoric or boric acid gave the same percentages of alpha alumina within the normal variation of duplicate runs. The conclusion was that phosphoric acid appeared as effective as boric acid in preventing the formation of alpha alumina.

Samples CJ-CM were designed to determine the effect of the individual fission products at 10 times their expected concentration. The samples with molybdenum and the rare earths did not form alpha alumina, so these elements may help prevent the formation of alpha alumina. The sample containing barium plus cesium and the one containing zirconium did form alpha alumina, which indicates that these either promoted the formation of alpha alumina or did not affect the formation of alpha alumina which is normal when sodium is present.

The possible effects of fission products on both the crystallinity of alumina and the effectiveness of boric acid were tested in samples ER to EV. The aluminas contained simulated fission products at zero, one, or two times the normal concentration, and two of the five aluminas also contained boric acid at a low concentration. The addition of fission products did not prevent formation of alpha alumina; in fact, sample EO with fission products had a higher alpha content than the control sample EP. Each of the two samples (EN and ER) which contained boron in addition to fission products had a lower alpha content than the adjacent sample without boric acid (EO and EQ). These results are consistent with the supposition that fission products at normal concentrations will not significantly affect the formation of alpha alumina nor interfere with the use of boric acid to control crystallinity.

Sample CW was a test of the effect of adding a stainless steel waste solution to an aluminum nitrate solution, and the formation of alpha alumina indicated that mixing the two wastes together would not reduce this formation.

The minimum temperature for formation of alpha alumina was studied by heating samples H, K, BB, and BC in the micro reactor. Samples K, 22PP, and IVA formed alpha alumina at 350°C and a lesser amount at 325°C. The literature[6] on hydrothermal transformations of alumina indicates 375°C as a minimum temperature for formation of alpha alumina, so the formation of alpha alumina at 325°C is a unique result. If a useful minimum temperature (e.g., 375°C) had existed for forming alpha alumina, then fluidization tests could be run in the pilot plant to determine whether such a minimum temperature applied to fluidization as well as hydrothermal experiments. These results are given in Appendices A, B, and C. The minimum temperature is probably too low to be useful in controlling alpha formation.

Aluminas BX to CC were prepared at a fairly low temperature as part of a study to look for new phases. The C-phase reported earlier[3] was also found in the synthetic aluminas (BX to BZ in Appendix B) prepared from acidic solutions. Samples BX to CC were heated at 250°C and 350°C in the micro reactor to study the possible formation of new phases. Tho results were not especially illuminating. The C-phase may be stable to 250°C, and no new phases were found.

B. Fluidized Calcination of Aluminum Nitrate Wastes

Owing to the lack of pilot plant data on fluidization of nitrates of stainless steel or Nichrome, tests were made using a two-inch-diameter fluidizer to determine the crystallinity of the product from a laboratory fluidizer. Solutions of aluminum nitrate were also run to obtain a reference sample and to gain experience in operating the fluidizer. The apparatus and description of the runs on aluminum nitrate are reported here, and the runs on stainless steel and nichrome are described in the appropriate sections below.

The compositions of the solutions are given in Table II, the operating conditions in Table III, the analyses of the products in Table IV, and the size distributions of the products in Table V.

Table II

SOLUTIONS USED FOR FLUIDIZATION

Run No.	Composition of Solution,[1] Molar						
	Al	Fe	Cr	Ni	HNO_3	F.P.	Other
F7	1.29				2.8		0.2 $NaNO_3$
F8		1.0			1.0		
F9	1.70				1.3	0.005	0.1 $NaNO_3$, 0.027 $Hg(NO_3)_2$
F10		1.5			1.0		
F11		1.12	0.26	0.12	1.0	0.005	
F12		1.12	0.26	0.12	1.0	0.005	0.15 H_3BO_3
F13a			0.27	1.23	1.0	0.005	
F13c			0.36	1.64	1.0	0.005	
F14			0.36	1.64	1.0	0.005	(0.3) H_3BO_3[2]

[1] Al = $Al(NO_3)_3 \cdot 9H_2O$, Fe = $(NO_3)_3 \cdot 9H_2O$, Cr = $Cr(NO_3)_3 \cdot 9H_2O$, Ni = $Ni(NO_3)_2 \cdot 6H_2O$. For 0.005 M F.P., the concentrations of fission products were $CsNO_3$ 0.0013, $ZrO(NO_3)_2$ 0.0012, $Na_2MoO_4 \cdot 2H_2O$ 0.0010, $La(NO_3)_3 \cdot 6H_2O$ 0.0006, $Ce(NO_3)_3 \cdot 6H_2O$ 0.0005, $Ba(NO_3)_2$ 0.0003, $RuCl_3$ 0.0003.

[2] Boric acid was added at 0.4 molar, but was incompletely dissolved.

Table III

OPERATING CONDITIONS FOR FLUIDIZATION EXPERIMENTS

Run[1]	Feed Solution[2]	Bed Temp. (°C)	Fluidization Air Velocity[3] (ft/sec)	Nozzle Air to Liquid Ratio[4]	Liquid Feed Rate[4] (ml/min)
F7a	Al	400	1.0	1500	0.77
F7b	Al	410	1.0-1.3	1600	0.82
F7c	Al	410	0.95	2100	0.72
F7d	Al	400	0.76	2300	0.69
F8	Fe	380	0.74	1500	1.00
F9a	Al	300	0.53	1600	1.26
F9b	Al	350	0.63	2000	0.88
F9c	Al	350	0.66	2000	1.33
F10a	Fe	300	0.58	1300	1.7
F10b	Fe	300	0.76	1300	1.3
F10c	Fe	300	0.82	1250	2.1
F11a	SS	350	0.62	2000	1.3
F11b	SS	350	0.52	1800	1.5
F11c	SS	400	0.76	2400	1.1
F12a	SS+B	350	0.62	2300	1.1
F12b	SS+B	350	0.41	1500	1.3
F12c	SS+B	350	0.60	1600	1.6
F12d	SS+B	350	0.62	2000	1.3
F12e	SS+B	350	0.62	2100	1.2
F13a	Nic	300	0.48	1100	2.1
F13b	Nic	350	0.52	1300	1.8
F13c	Nic	400	0.48	1700	1.1
F13d	Nic	400	0.47	1800	1.1
F13e	Nic	400	0.48	1800	1.3
F14a	Nic+B	400	0.48	1900	1.1
F14b	Nic+B	400	0.48	2000	1.0
F14c	Nic+B	400	0.48	1600	1.2
F14d	Nic+B	400	0.55	1800	0.9
F14e	Nic+B	400	0.62	2100	0.8

[1] The small letters a, b, c, etc., refer to successive days of operation with the same feed solution.

[2] See Table II for composition.

[3] Fluidizing air velocity calculated for a column temperature of 400°C and atmospheric pressure.

[4] Nozzle air calculated at nozzle pressure and 25°C. Liquid rate calculated from volumetric measurement.

Table IV

SAMPLES FROM FLUIDIZATION EXPERIMENTS

Run	Description	Grams	LOI[1] (%)	X-ray Data[2]
F7c	Bed	--	11.9	--
F7d	Bed	--	11.9	--
F7d	Overhead	--	32.6	$NaNO_3$(67)
F8	Bed	--	1.3	α-Fe_2O_3(136)
F8	Overhead		4.3	α-Fe_2O_3(103)
F9c	Bed	79	13.4	--
F9c	Overhead	25	48.3	$Al(NO_3)_3 \cdot 9H_2O$? (23)
F10c	Bed(-10 mesh)	81	1.1	α-Fe_2O_3(23)
F10c	Bed(+10 mesh)	25	0.6	α-Fe_2O_3(156)
F10c	Overhead	22	7.5	α-Fe_2O_3(90)
F11b	Bed	--	1.0	α-Fe_2O_3(48)
F11c	Bed	110	1.0	α-Fe_2O_3(55),2.94(3)
F11c	Overhead	16	9.1	α-Fe_2O_3(20)
F12d	Bed	117	2.0	α-Fe_2O_3(21)
F12d	Overhead	19	11.0	α-Fe_2O_3(11)
F12e	Bed	104	2.0	α-Fe_2O_3(21),2.94(2)
F12e	Overhead	5	8.3	α-Fe_2O_3(13),2.94(2)
F13cde	Bed	60	2.4	NiO(59),2.50(4),2.93(2)
F13e	Overhead	46	19.2	NiO(38)
F14cde	Bed	103	3.4	NiO(24)
F14c	Overhead	23	15.9	NiO(23)
F14e	Overhead	19	17.9	NiO(19),2.53(2)

[1] LOI = Loss on ignition at 1000°C.

[2] Phases or unidentified lines are followed by intensity in recorder divisions (enclosed in parentheses).

Table V

SIZE DISTRIBUTION OF PRODUCTS FROM FLUIDIZATION RUNS

Run	Feed Solution	Percent Retained on Screen				
		+20	+40	+60	+100	-100
F9	Al	43	43	11	2	
F10	Fe	18	55	20	6	1
F11	SS	47	41	10	2	
F12	SS+B	31	47	14	6	1
F13	Nic	6	66	22	5	1
F14	Nic+B	15	47	27	9	1

Run F7 with aluminum nitrate and run F8 with ferric nitrate were made using the two-inch fluidizer used earlier.[3] A new nozzle was built which could use air at pressures of 30 psig. The nozzle consisted of 21-gauge hypodermic tubing for the liquid, with a concentric 16-gauge hypodermic tube for air.

Run F7 extended over a period of 4 days. The first day (F7a) did not produce much product, but showed no signs of caking. The second day started with 44 g of charge (-10 + 40 mesh) and had some caking during the run as shown by evolution of fumes when the bed was stirred. The third day (F7c) started with 25 g of bed but this was lost during the morning. Extra bed material was added, and then the fluidizer operated satisfactorily. The fourth day (F7d) was satisfactory.

After run F8 with ferric nitrate, the Vycor tube of the fluidizer was rebuilt, using 2.25-inch-ID tubing rather than the 1.75-inch. A porous stainless steel frit was used for the fluidizer and the nozzle was placed about one-half inch above the frit. The nozzle was the same type as before except that a slightly larger annular space for the nozzle air was obtained by using tubing with an inside diameter of 0.0425-inch in place of 0.041-inch.

Run F9 was made using an aluminum nitrate solution containing simulated fission products, mercuric nitrate, and sodium nitrate. The apparatus was operated for three days, starting with 40 cc (39 g) of -20 + 60 mesh material from the pilot plant at Idaho Falls (Sample 22PP-04-0430). The first day (F9a) produced considerable caking. The second day (F9b) was started with fresh bed material and operated satisfactorily. The third day (F7c) was started with the bed material from the previous day, and the operation was good. The particles had grown considerably in size and were spherical; their appearance was much better than anything produced previously in our laboratory.

C. Differential Thermal Analysis of Aluminum Nitrate

Differential thermal analysis (DTA) is useful for studying chemical reactions or phase changes in a sample while it is heated continuously to a high temperature. The same apparatus was used as before.[3] For most of the runs, the samples were heated from room temperature to 800°C in air, while a few runs were made with an atmosphere of nitrogen dioxide.

The purpose of the DTA was to study the reaction of boric acid and sodium nitrate with alumina and aluminum nitrate. Aluminum nitrate must be mixed with at least 50% of aluminum oxide so the sample will not sink below the thermocouple when the aluminum nitrate melts at 70°C. The results are given in Table VI and a few DTA curves are shown in Figure 1. All of the curves in Figure 1 were for runs with an atmosphere of air, but a few of the samples (see Table VI) were run with nitrogen dioxide flowing through the tube.

Table VI

DIFFERENTIAL THERMAL ANALYSIS OF ALUMINUM COMPOUNDS WITH BORIC ACID AND SODIUM NITRATE

Sample[1]	Gas	Peak Temperatures and Magnitudes[2]
B(18%)+AlO(82%)[3]	Air	168°(-8.5),183°(-3.2),204°(-1.7)
B(18%)+IV A(82%)[3]	Air	S135°(-2.8),168°(-6.2),676°(+2.0),739°(-1.0)
NaN(12%)+AlO(88%)	Air	321°(-3),S714°(-3),756°(-3.4)
NaN(12%)+IV A(88%)	Air	282°(-0.2),306°(-1.8),613°(-1.3)
B(15%)+NaN(10%)+ Al°(83%)[3]	Air	183°(-8.5),330°(-1.8),593°(+0.7),700°(-5.0)
B(30%)+NaN(20%)+ AlO(50%)	Air	187°(-11.5),320°(0.2),358°(-3.8),647°(+1.5)
AlN(45%)+AlO(55%)[3]	Air	92°(-9.0),S116°(-6.2),180°(-22),S251°(-2.7)
AlN(50%)+AlO(50%)	Air	94°(-8.6),S116°(-4.5),183°(-20),S242°(-6?)
AlN(41%)+B(9%)+ AlO(50%)	Air	92°(-10.5),S148°?(-13°?),187°(-32),S230°(-4.2)
AlN(43%)+NaN(5%)+ Al°(52%)[3]	Air	S90°(-6.8),96°(-8.3),166°(-10.2),312°(-0.7),701°(-1.4)
AlN(46%)+NaN(2%)+ AlO(52%)	Air	96°(-14.5),132°(-5.2),S160°(-7.0),170°(-8.4),241°(-0.2)
AlN(40%)+B(8%)+ NaN(5%)+AlO(47%)[3]	Air	89°(-10.5),S107°(-7.5),163°(-8.8),311°(-0.4)
B(18%)+AlO(82%)	NO_2	80°(-0.2),163°(-7.6),177°(-3.0),199°(-1.3)
D(18%)+IV A(82%)	NO_2	52°(-1.3),160°(-10)
AlN(50%)+AlO(50%)	NO_2	?43°(-0.8),90°(-7.0),188°(-18.5),S254°(-2.5°),386°(-0.3)
AlN(41%)+B(9%)+ AlO(50%)	NO_2	67°(-2.5),170°(-5.4),219°(-0.3)
AlN(48%)+NaN(2%)+ AlO(50%)	NO_2	90°(-7.0),111°(-5°),179°(-14),S272°(-1°)
AlN(47%)+B(1.6%)+ NaN(1.1%)+AlO(50%)	NO_2	57°(-1.5),91°(-12.5),S119°(-8),159°(-8°),278°(-0.4)

[1] AlN = $Al(NO_3)_3 \cdot 9H_2O$, B = H_3BO_3, NaN = $NaNO_3$, AlO = αAl_2O_3 (inert)
IV A = amorphous alumina from pilot plant.

[2] Peak temperature is followed by the differential temperature (Δt enclosed in parentheses). An "S" before the temperature denotes a shoulder on the side of a larger peak.

[3] DTA curve also given in Figure 1.

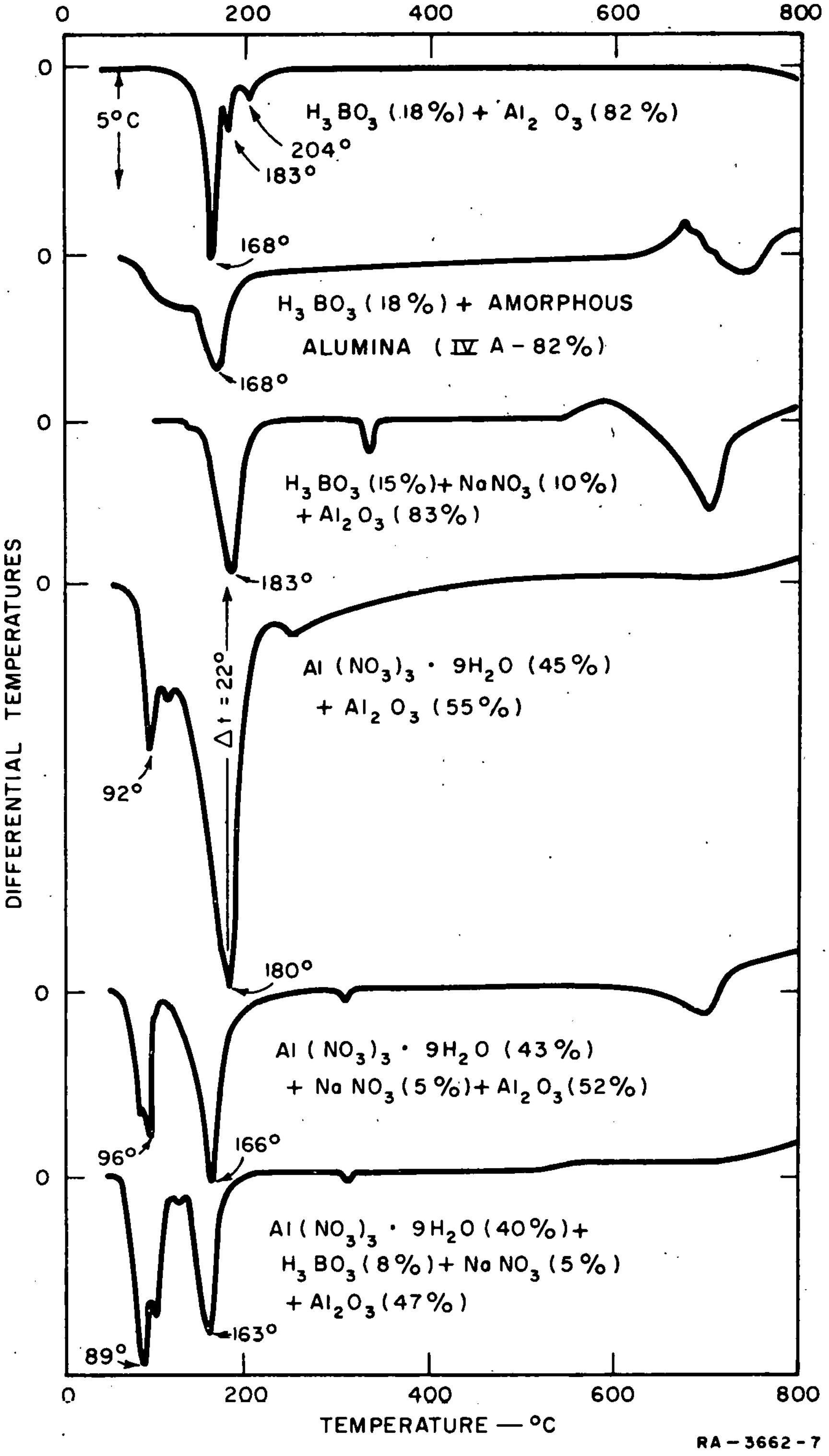

FIG. 1. DTA OF ALUMINUM COMPOUNDS WITH BORIC ACID AND SODIUM NITRATE

Boric acid diluted with aluminum oxide had three peaks, at 168, 183, and 204°C, while the same concentration of boric acid in amorphous alumina (pilot plant sample IV A) had only one peak, at 168°C. The absence of the boric acid peaks at 183 and 204°C indicates that amorphous alumina reacts with boric acid below 183°C.

Sodium nitrate had its main peak at 321°C, while sodium nitrate mixed with amorphous alumina had a smaller peak at 306°C. This may indicate a partial reaction of sodium nitrate with amorphous alumina below 320°C.

A mixture of boric acid and sodium nitrate diluted with aluminum oxide had its first peak at 183°C, and the absence of the boric acid peak at 168°C indicates that sodium nitrate and boric acid react below 168°C.

The DTA of aluminum nitrate is quite complex. Therefore, the differences between the DTA of aluminum nitrate alone and with additions of boric acid or sodium nitrate are difficult to interpret. The first main peak of aluminum nitrate was observed at 90 to 96°C and differences appear in the shape of the peak. The second main peak which normally appeared at 180° was found at 163 to 170°C if sodium nitrate was present, while addition of boric acid had no obvious effects on the DTA of aluminum nitrate.

The last six runs in Table VI were made in the presence of nitrogen dioxide. Boric acid alone and added to amorphous alumina (IV A) acted similarly to the runs with air, indicating that amorphous alumina can react with boric acid below 180°C. The addition of boric acid or sodium nitrate lowered the temperature of the second main peak of aluminum nitrate.

Thermogravimetric studies were made at Idaho Falls[7] with mixtures of boric acid and sodium nitrate. Sodium nitrate alone had no loss up to 650°C while boric acid lost water in the region from 90 to 300°C to form boric oxide. The mixtures showed a plateau corresponding to the formation of boric oxide in the region from 250 to 400°C, while X-ray diffraction indicated some metaboric acid and sodium nitrate. A second plateau at 475 to 575°C gave X-ray diffraction patterns showing sodium nitrate and small amounts of metaboric acid and sodium perborate ($Na_2B_2O_5 \cdot 2H_2O$). The weight losses corresponded to the formation of sodium polyborates. Finally, above 575°C, the curves became complex and included the decomposition of sodium nitrate. The data indicated interaction of sodium nitrate and boric acid below 400°C.

D. Pot Calcination of Aluminum Wastes

During the evaporation of some of the aluminum nitrate solutions in Appendix A, it appeared that certain additives had significant effects on the evaporation and the bulk density of the product. Additives seemed worth testing to determine their usefulness for aiding pot calcination, and tests were made with solutions in beakers. The mole ratios of the additives to aluminum nitrate were 0.24 to 0.72 H_3PO_4, 0.4 to 0.8 H_3BO_3, 0.5 $Na_3PO_4 \cdot 12\ H_2O$, 0.5 $NaNO_3$, 0.5 to 1.0 Na_2SO_4, 0.5 Na_2CO_3, 0.5 NaOH, 0.25 $Na_2SiO_3 \cdot 9\ H_2O$, and 0.5 to 1.5 H_2SO_4. The solutions were heated on a hot plate until solids began to appear, and the volume was measured. Then the mixtures were heated in a muffle furnace at 300°C and a final volume was determined. Phosphoric acid was the best additives in giving the highest bulk density of the final solids, but in one series it appeared poorer than the control. The optimum concentration was at 0.6 mole of phosphoric acid per mole of aluminum nitrate, which may correspond to a "eutectic" between the aluminum phosphate and alumina. These tests were essentially qualitative in nature, and indicate that further laboratory studies should be made, using phosphoric acid as an additive for pot calcination. All of the other additives were poorer than the control.

E. Transformation Studies on Pilot Plant Samples

Samples from the 2-foot-square unit and the DWCF were used to study phase transformations, the acid insoluble material from amorphous alumina, the nature of boron in alumina by extraction experiments, and location of crystalline phases in particles by electron diffraction and photomicrographs of particles. A list of the samples used for these purposes is given in Table VII.

Table VII

ALUMINAS RECEIVED FROM IDAHO FALLS

Sample[1,2]	Bed Temp. (°C)	Mole Ratios to Al_2O_3				X-Ray Data[4]
		Na_2O[3]	H_2O	NO_3^-	B_2O_3[3]	
23B-P-26-1230	400	0.060	0.49	0.14	0.16	α(7%),$NaNO_3$(3)
23B-XJP-26-1230	400	0.060	0.80	0.19	0.16	--
24-P-08-0830	400	0.060	0.48	0.17	0.04	α(10%)
24-XJP-08-0930	400	0.060	0.70	0.21	0.04	--
27-P-26-0830	400	0.155	0.61	0.22		α(28%)$NaNO_3$(38), 3.36(11)γ(8)
27-JP-26-0830	400	0.155	0.32	0.36		α(12%)$NaNO_3$(54), γ(8)
27-PX-28-1030	550	0.155	0.12	0.14		α(39%),$NaNO_3$(33), Iota (27)
27-JPP-28-1430	550	0.155	0.11	0.17		α(3%),$NaNO_3$(48), Iota (107)
27B-P-30-1630	400	0.060	0.13	0.09	0.08	α(3%),$NaNO_3$(6), 2.51(11)
27B-JP-30-1630	400	0.060	0.17	0.12	0.08	$NaNO_3$(4), 2.51(4)
28B-P-13-1230	400	0.060	0.19	0.17	0.01	α(1%)
28B-JP-13-1230	400	0.060	0.24	0.18	0.01	--
DWCF005-1105		0.020	0.27	0.06	0.16	α(35%),2.80(19),3.36(10)
DWCF005-1110		0.020	0.31	0.07	0.16	α(17%),3.36(4)
DWCF005-1115		0.020	0.20	0.07	0.16	α(10%)
DWCF009-0703		0.020	0.10	0.03	0.01?	α(85%),3.36(8),$NaNO_3$(5)
DWCF009-0712		0.020	0.13	0.03	0.01?	α(86%),3.36(93),$NaNO_3$(5)
IVA		0.060	0.55	0.16		α(9%),γ(2),3.24(2)
22PP-09-0430		0.060	0.43	0.22		α(1%),$NaNO_3$(5)

[1] P = product; JP, JPP, or XJP = overhead fines.

[2] Normal composition of feed was 1.29 M aluminum nitrate, 2.34 M nitric acid, 0.078 sodium nitrate, and 0.015 M mercuric nitrate.

[3] Calculated from feed concentrations.

[4] Alpha contents are reported in percent. Other phases or unidentified lines are followed by the intensity in arbitrary scale divisions (enclosed in parentheses). C = C phase, Iota = Iota Al_2O_3.

The samples from runs 23 to 28, from the 2-foot-square calciner, were heated in a tube furnace at 500°C in an atmosphere containing nitric acid and water vapor. Very little change in the X-ray diffraction patterns resulted from the heating; the alpha contents did not increase significantly. The peaks due to sodium nitrate decreased, and the X-ray peaks due to iota alumina (27PX and 27 JPP samples) increased. The results are given in Appendix D.

Iota alumina is an interesting form of alumina within an X-ray pattern similar to that of mullite, $3Al_2O_3 \cdot 2SiO_2$. Iota alumina has been reported[8] to be formed by rapid quenching of cryolite-alumina melts and to transform through eta alumina to alpha alumina on heating. The pilot plant samples containing iota alumina had a high sodium content (0.2M sodium nitrate in the feed compared with tne usual 0.078M) and a high bed temperature (550°C). Possibly the iota alumina formed in the pilot plant contain sodiums or differs in composition from the iota alumina reported by Foster.[8]

The pilot plant samples from Idaho Falls were also heated in the micro reactor under moderate pressure, and the results are given in Table VIII. Aluminum borate ($9Al_2O_3 \cdot 2B_2O_3$) was found in the samples containing 0.08 mole (or more) B_2O_3 per mole of Al_2O_3; it was absent from the samples containing 0.04 mole or less. All samples containing α-Al_2O_3 showed an increase in the α-Al_2O_3, and a decrease in the iota alumina (in the aluminas formed at 550°C). If one were to postulate a phase diagram for the system at equilibrium, then the α-Al_2O_3 region would extend to about 0.06 mole B_2O_3 per mole Al_2O_3, and a two-phase region containing α-Al_2O_3 and $9Al_2O_3 \cdot 2B_2O_3$ might extend to 0.22 mole B_2O_3 per mole of Al_2O_3. However, in the ordinary product from fluidization, the boron and aluminum atoms are randomly distributed throughout a network of oxygen atoms, and the over-all structure is mainly amorphous. The optimum concentration of boron might be between 0.01 and 0.06 mole B_2O_3 per mole of Al_2O_3 to control the formation of alpha alumina.

Table VIII

ALUMINAS FROM IDAHO FALLS HEATED IN MICRO REACTOR

Sample[1]	Heating Conditions			Product-Mole Ratios to Al_2O_3			X-Ray Data[3]
	Temp, (°C)	Pressure (psig)	Time (hr)	H_2O	NO_3	Other[2]	
23B-P-26	430	90	165	0.19	0.076	Na,B	α(9%),$NaNO_3$(16),AlB(70)
23B-XJP-26	430	90	165	0.23	0.092	Na,B	γ(5),$NaNO_3$(23),AlB(74)
24-P-08	430	120	160	0.18	0.111	Na,B	α(35%),$NaNO_3$(34),γ(7)
24-XJP-08	430	120	160	0.33	0.119	Na,B	γ(5),$NaNO_3$(33),A(17)
27-P-26	430	120	160	0.22	0.253	Na	α(42%),$NaNO_3$(50),γ(7) 3.36(24)
27-JP-26	430	120	160	0.52	0.388	Na	α(27%),$NaNO_3$(56),γ(7)
27-PX-28	430	90	165	0.17	0.219	Na	α(53%),$NaNO_3$(53),Iota(9)
27-JPP-28	430	90	165	0.33	0.223	Na	α(16%),$NaNO_3$(56),Iota(49)
27B-P-30	430	90	165	0.19	0.052	Na,B	α(4%),γ(7),$NaNO_3$(11),AlB(42)
27B-JP-30	430	90	165	0.18	0.067	Na,B	γ(10),$NaNO_3$(13),AlB(28)
28B-P-13	430	120	160	0.08	0.117	Na,B	α(83%),$NaNO_3$(30)
28B-JP-13	430	120	160	0.05	0.130	Na,B	α(96%),$NaNO_3$(55)

[1] See Table VII for original composition.

[2] Compositions of other elements are the same as in Table VII.

[3] Alpha contents are reported in percent. Other phases or unidentified lines are followed by the intensity in arbitrary scale divisions (enclosed in parentheses). C = C phase, Iota = Iota alumina, AlB = $9Al_2O_3 \cdot 2B_2O_3$, γ = gamma alumina.

F. Bonding of Boron in Alumina

The role of boron in retarding formation of alpha alumina and the possible volatilization of boron from alumina may depend on the bonding of boron in the alumina. One possibility is that boron combines with sodium and prevents the sodium from promoting the formation of alpha alumina. Another possibility is that the boron is bonded to oxygen atoms which are randomly bonded to other boron or aluminum atoms, and that the irregular network structure hinders the formation of a regular crystal structure. If the boron were combined with sodium, a water extraction might remove a significant fraction of the boron without altering the alumina; while boron in a network of oxygen and aluminum atoms should not be so easily extracted.

Four samples from the pilot plant, one from the Demonstration Waste Calcining Facility (DWCF), and five samples of synthetic alumina were used. After preliminary tests, 2-gram samples (-100 mesh) were extracted with 25-ml portions of water by boiling for 1/2-hour. The mixture was filtered into 100-ml volumetric flasks, and aliquots were used for the analyses.

Boron was determined by the mannitol method after neutralizing with standard 0.1N NaOH to the methyl red endpoint. If aluminum was present the sample was heated to boiling during the neutralization. The mannitol was added and the sample titrated to the phenolphthalein endpoint. The boron was corrected for a slight interference from aluminum. Aluminum was determined by precipitating aluminum hydroxide on a separate aliquot. Nitrate was determined by the dichromate method. Sodium was determined by flame photometry.

The amount of boron and aluminum extracted was calculated as a percentage of the amount originally present, and the results are given in Table IX. From these results, water seemed to extract about half of the boron. However, the boron could be "extracted" by hydrolysis of the sample according to the hypothetical equations:

Table IX

EXTRACTION OF BORON FROM ALUMINAS

Sample	Extract[1]	Original Composition (%)			Extraction (% of Original)			Mole Ratio, Na/B
		Al_2O_3	NO_3^-	B_2O_3[2]	Al_2O_3	B_2O_3	Na	
23BP-26-1230	H_2O	77.1	6.36	8.44	--	38	69	0.7
	C_2H_5OH				--	1	5	1.3
23BXJP-26-1330	H_2O	72.6	8.41	7.95	--	58	93	0.6
	C_2H_5OH				--	1		
24P-08-0830	H_2O	81.4	8.21	2.22	--	11	83	11
	C_2H_5OH				--	4	5	5
27BP-30-1630	H_2O	86.5	4.48	4.73	--	48	74	1.1
	C_2H_5OH					3		
DWCF-005-1105	H_2O	81.5	3.24	8.92	--	35	68	1.0
	C_2H_5OH				--	2	5	
AX[3]	H_2O	65.8	20.1	4.50	40	48	--	--
	C_2H_5OH				--	2	--	--
F-11[4]	H_2O	81.7	8.78	2.07	--	35	76	1.3
	C_2H_5OH				--	1		
CD[3]	H_2O	46.6	29.5	14.7	64	76	91	0.2
	C_2H_5OH				--	4		
CE[3]	H_2O	56.6	21.8	3.48	21	31	100	2.1
	C_2H_5OH				--	2		
CX[3]	H_2O	63.2	21.9	8.98	2	35	86	3.5
	C_2H_5OH				--	6	98	20

[1] 2 g were boiled with 25 ml of H_2O for 1/2-hour or with ethanol for 5 minutes.

[2] Calculated from composition of feed solution.

[3] Synthetic aluminas prepared by the boil-down method at SRI.

[4] Synthetic aluminas prepared by the 2-inch fluidizer at SRI.

$$Al_xB_yO_3 + 3H_2O \rightarrow xAl(OH)_3 + yH_3BO_3 \; ; \; x + y = 2$$

$$Al_xB_y(OH)_{6-x}(NO_3)_x \rightarrow xAl(OH)_2^+ + yH_3BO_3 + xNO_3^- \; ; \; x + Y = 2$$

Thus the "extraction" of boron by water doesn't necessarily indicate the form of boron in the alumina.

To avoid the difficulty from hydrolysis, tests were then made with methanol at room temperature and with ethanol heated to boiling. About 1% of the boron was extracted by ethanol on sample F-11. On sample CD, water extracted about 20% of the boron, methanol extracted 2%, and ethanol (hot) extracted 4%. The solubility of boric acid in ethanol is more than twice that in water, so the high "extractions" with water were probably due to hydrolysis. All of the samples were then extracted with ethanol by boiling 2-g portions with 25 ml of ethanol for 5 minutes, letting stand while hot for 10 minutes, and then filtering.

The percentage of the original boron extracted by ethanol varied from 1 to 6%, with no particular correlation between the amount of original boron and the amount extracted. These results indicated that the bulk of the boron was probably randomly distributed with aluminum atoms in a network of oxygen atoms (e.g., -O-B-O-Al-O-), similar to the structure of glasses,[3] rather than being present as free boric acid or a sodium borate. The experiments in which phosphoric acid was found to be as effective as boric acid would be explained by this same type of bonding, while the formation of sodium compounds might require differing ratios of boric acid and phosphoric acid for the same effectiveness.

An average of 84 percent of the sodium was "extracted" by water. About 5% of the sodium was extracted by ethanol, except for sample CX, which had a very large extraction and a much higher sodium content. The mole ratios of sodium to boron (see Table I) varied considerably and didn't indicate a definite sodium borate. Probably the sodium and boron are extracted independently of each other. The results for sodium could support the idea that most of the sodium is bonded to alumina rather than to nitrate ion.

G. Electron Diffraction and Microscopic Examination of Pilot Plant Samples

Electron diffraction studies were made on two DWCF samples and two pilot plant samples from runs containing boron in the feed. The purpose was to determine if the particles were distinctly different from those examined earlier.[3] The particles were mounted and cut to obtain wedge-shaped samples so the particles could be examined along a line through their centers. Photographs of the electron diffraction patterns were taken at five locations; at the outer edges (r), at the center, and at the midpoints (r/2).

The results are given in Table X, with each line representing a single particle. The particles from the two DWCF samples were mainly amorphous. A minor amount of alpha alumina was found in two of the particles of DWCF-005-1110, and an unidentifiable single crystal pattern was found in one particle. Sample 27P-26 had a random distribution of alpha alumina with the most intense patterns occurring at the outer edge of some particles and at the center of other particles. Sample 27PX-28 also had a random distribution of alpha alumina, and two particles were amorphous. The results do not alter the conclusion from the earlier tests[3] that alpha alumina forms uniformly in a portion of the particles (not necessarily at the center or edge) and not randomly in very small spots distributed through the particle.

Microscopic examination was made on many of the pilot plant samples in Table VII. The particles were mounted in transparent plastic and polished as in preparation of metallographic samples. The cross-sectioned particles were examined with a binocular microscope and photomicrographs were taken of the samples at 18 x and 90 x magnification. Two samples are shown in Figure 2, DWCF 005-1110 and DWCF 009-0703. The 005-1110 sample shows a normal particle and an agglomerate of several particles, which occurred infrequently. The normal particle has a fairly solid appearance and concentric rings are noticeable mainly by shading. The agglomerate type of particle was discussed in the earlier technical

Table X

ELECTRON DIFFRACTION ALONG DIAMETERS OF PARTICLES

Sample	Electron Diffraction[1]					Diam. (mm)
	Edge	r/2	Center	r/2	Edge	
DWCF-005-1110	a	a	a	α_{w}	α_{m}	1.0
	a	S_{w}	s_{vw}	a	a	0.9
	a	α_{vw}	a	a	a	1.0
	a	a	a	a	a	0.5
	a	a	a	a	a	0.5
DWCF-005-1115	a	a	a	a	a	0.8
	a	a	a	a	a	0.5
	a	a	a	a	a	0.4
	a	a	a	a	a	0.7
	a	a	a	a	a	0.5
27-P-26	α_{w}	α_{m}	α_{vw}	α_{vw}	α_{m}	0.5
	α_{m}	α_{s}	α_{m}	α_{m}	α_{s}	0.3
	α_{vw}	α_{m}	α_{w}	α_{vw}	α_{m}	0.3
	$\alpha_{w+S_{w}}$	α_{w}	a	α_{vw}	α_{vw}	0.3
	α_{w}	a	α_{w}	a	a	0.3
27-PX-28	a	α_{vw}	α_{m}	α_{w}	a	0.5
	S_{w}	a	a	a	a	0.3
	a	a	a	a	a	0.3
	a	a	a	a	a	0.5
	α_{w}	α_{vw}	α_{vw}	a	α_{vw}	0.3

[1] Electron diffraction reported on 5 locations for single particles. The identification is followed by a rough indication of the intensity of the pattern: s = strong, m = medium, w = weak, and vw = very weak and uncertain. a = amorphous or no pattern. α = alpha alumina, S = single crystal pattern.

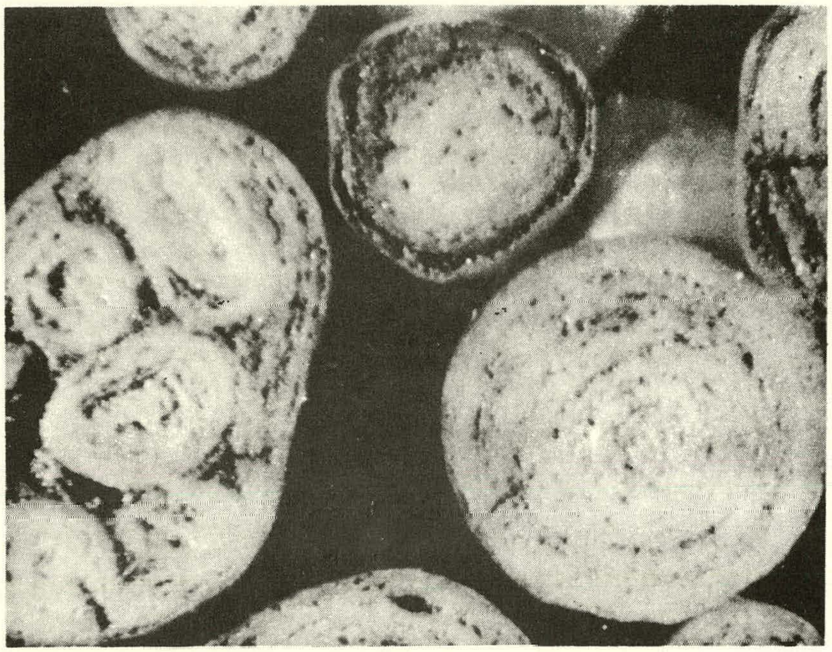

(a) DWCF 005 – 1110 AT 90 X

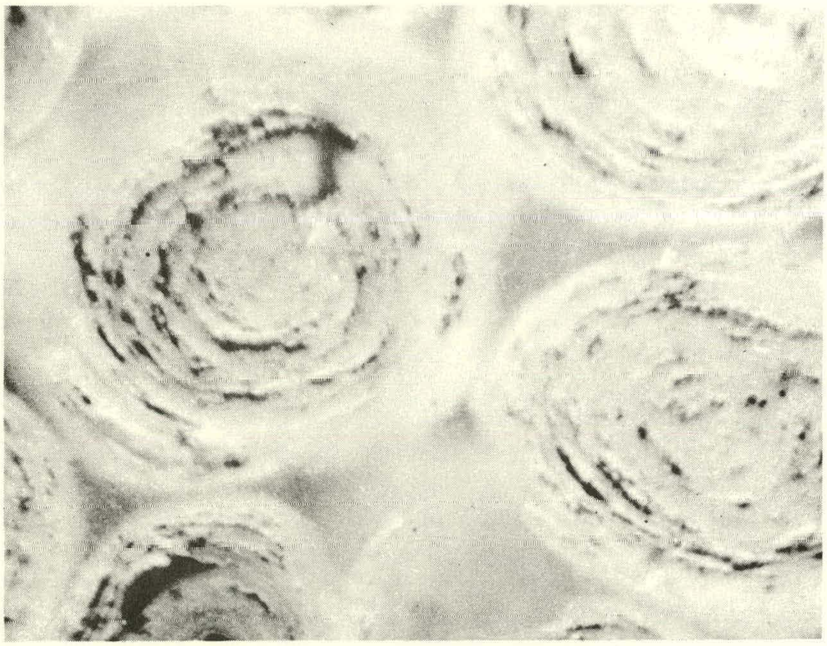

(b) DWCF 009 – 0712 AT 90 X

RP 3662-9

FIG. 2 PHOTOMICROGRAPHS OF FLUIDIZED ALUMINA report. The particles in DWCF sample 009-0703 had a high alpha alumina content and the concentric rings are more easily seen; they may represent a physical separation of the concentric layers. Several pilot plant samples were arranged in order of increasing ease of discerning the concentric layers. Some consideration was also given to the fraction of particles which had lost their central portions during the preparation of the mounted samples. The arrangement of the samples, with the percent of alpha alumina in parentheses, was as follows: DWCF 005-1115 (10% α), 24-P-08 (10% α), 27B-P-30 (3% α), 23B-P-26 (7% α), DWCF 005-1110 (17% α), 28B-P-13 (1% α), DWCF 005-1105 (35% α), 27-P-26 (28% α), 27-PX-28 (39% α), DWCF 009-0703 (85% α), DWCF 009-0712 (86% α). The order of arrangement on the basis of physical appearance is good but not in perfect agreement with the alpha alumina content. Increased separation of layers with increase in percentage of alpha alumina is in the direction that one would expect if amorphous alumina of density less than 3.0 should shrink to alpha alumina with a density of 4.0.

The only other noteworthy observations were that samples 27-P and 27-PX contained many particles with transparent to reddish glassy material at their centers, possibly due to use of sand as a bed material. Sample 27B-P had a distinct reddish band near the center of all of the particles and also contained a few agglomerates.

H. Acid Insoluble Fraction from Amorphous Alumina

Tests at Idaho Falls[4] have shown that alpha alumina is insoluble in hot 4 N nitric acid, while amorphous alumina is soluble. In applying this method to the IV A sample of amorphous alumina at Idaho Falls, the residue had an analysis of 82% alpha alumina by X-ray diffraction. The residue amounted to about 8% of the starting material. Electron diffraction was to be applied at Stanford Research Institute to this residue to determine the nature of the portion of the sample which was not alpha alumina (i.e., the remaining 18%).

The residue from Idaho Falls was separated into light and heavy fractions, using a solution of thallium malonate and thallium succinate.

Residues of the acid insoluble fraction of samples IV A and 22 PP were also prepared at Stanford Research Institute. The liquid was adjusted to a specific gravity of 3.8, which was selected to allow alpha alumina (sp. gr. 3.98) to sink, while gamma alumina (sp. gr. < 3.6) and other aluminas would float. A sample of the residue was placed in a 50-ml graduate, mixed, and allowed to stand overnight. The top portion of the suspension was removed, filtered on a Millipore filter, and washed. It appeared that some particles floated which were fairly large and may have consisted of agglomerates containing voids. The residue prepared at Idaho Falls was ground to -100 mesh and the thallium solution was adjusted to a specific gravity of 3.6 for one separation and to 3.7 for a second separation.

The light fractions varied from 15 to 23 percent of the sample, using a specific gravity of 3.8. The light fraction, using the 3.6 sp. gr. liquid, was only 1.6% of the sample, and the fraction using the 3.7 sp. gr. liquid was 7%. X-ray diffraction patterns were obtained on all of the fractions with a camera, but all of the patterns appeared the same with strong lines of alpha alumina and no other diffraction lines. The light fraction from the IV A sample (3.6 sp. gr.), and the light fraction from the 22 PP sample (3.8 sp. gr.) and the heavy fraction from the IV A sample were also run using electron diffraction. Several films were made of each of these samples. All films showed only alpha alumina and no other diffraction lines. The conclusion is that alpha alumina is the only identifiable phase in the acid-insoluble samples from amorphous alumina.

A secondary problem is the accuracy of analysis of alpha alumina in an amorphous alumina. Our X-ray analysis of the IV A sample gave a result of about 9%, and the product of the percent residue (8.4) times the percent alpha in the residue (75) was 7.5%. For sample 22 PP, the percent alpha in the original sample was barely detectable and a figure of 1% was reported. The product of the percent residue (2.5) times the percent alpha in the residue (75) was 1.9 percent. Thus, the X-ray analysis of low amounts of alpha in alumina is within 1 to 2%.

For high percentages of alpha alumina, the accuracy of the analysis based on the product of the peak height times the half width can be poor when large differences exist in crystallite size between the standard and the sample. The crystallite size as determined from line broadening was > 0.5 microns diameter for the Alcoa sample 5610, while the 90% alpha sample (from the Pilot Plant) had a crystallite size of 0.09 microns. The acid insoluble residues had crystallite sizes of 0.05 microns for the IV A residue and 0.04 microns for the 22 PP residue. These crystallite sizes are sufficiently different that a correction (if permissible) for the use of mixed Cu radiation[9] (i.e., the $K\alpha_1$ $K\alpha_2$ doublet) would increase the percent alpha in the acid insoluble residues from 75 to 93%. The two possible conclusions are that the acid insoluble residue either contains amorphous material which is not extracted by the 4 N nitric acid or contains only alpha alumina with a low analysis owing to the effect of crystallite size.

IV PHASE TRANSFORMATIONS IN CALCINATION OF NITRATES OF STAINLESS STEEL

In addition to processing wastes containing aluminum nitrate, fluidized calcination is useful to process stainless steel (type 304) or nichrome (80 Ni/20 Cr) wastes. A short test was made at Idaho Falls[10] on fluidized bed calcination of stainless steel wastes, using a 6-inch calciner. No special problems appeared, and a bulk density of 98 lb/cu ft was achieved.

The properties of hydrates and oxides of iron[11] can be compared with those of aluminum to relate the background obtained on alumina to calcination of stainless steel wastes. The iron hydrate goethite ($\alpha FeOOH$ or $Fe_2O_3 \cdot H_2O$) has the same crystal structure as diaspore, but goethite is formed by slow hydrolysis of iron salts while diaspore requires hydrothermal conditions of 2000 psi between 275 and 425°C.[6] Goethite can transform directly to αFe_2O_3 (hematite) and can also be formed by rapid hydrolysis of iron salts (e.g., boiling during hydrolysis), while α-Al_2O_3 requires hydrothermal conditions at 450° or above. α-Fe_2O_3 is also formed by a transition of γ-Fe_2O_3 at 400°, while the corresponding transformation of alumina is at 1050°C.

The properties of hydrates and oxides of chromium are less well defined, and α-CrO_3 is less easily formed than α-Fe_2O_3. The temperature for hydrothermal formation[12] of α-Cr_2O_3 is 450°C, about the same as for α-Al_2O_3. Chromium does not form a hydrate with the same crystal structure as diaspore[12] or a gamma type of oxide, but the α-Cr_2O_3 has the same crystal structure as α-Fe_2O_3 and α-Al_2O_3, and it can form solid solutions[13] with iron oxide or aluminum oxide.

Milligan and others have reported that composition ranges exist in which crystallization is hindered and which are designated as zones of mutual protection against crystallization. This was reported[14] to occur for the Cr_2O_3-Fe_2O_3 system at 20-70 mole percent of Cr_2O_3 up to 350°C. A similar effect was reported[15] in which the temperature for crystallization of α-Fe_2O_3 increased from about 140°C for pure iron hydroxide to 400°C at 24 mole % Al_2O_3. Various substances were reported[16] to hinder the transformation of amorphous ferric hydroxide to goethite (α-$Fe_2O_3 \cdot H_2O$), the most effective ones being AsO_2^-, glycerol, SiO_3^{-2}, and Al^{+3}. About 1% of silica sol retarded the crystallization of pure chromic oxide.[14]

A. Transformations in Stainless Steel Wastes

The transformations occurring with stainless steel wastes were studied in the same manner as for the alumina studies. Synthetic oxides were prepared from solutions of the nitrates, and these synthetic oxides were heated under pressure. The studies included the effect of additives, such as boric acid, phosphoric acid, alumina, rare earths, and fission products.

The compositions of the solutions are given in Table XI. These solutions were evaporated nearly to dryness and heated in a muffle at 230 to 290°C. At that temperature, the X-ray diffraction patterns of most of the oxides were amorphous or contained unidentified components with their most intense lines at d-values of 3.31 or 3.20. The only two samples with alpha iron oxide were the pure iron sample and the iron-nickel sample.

Each of the synthetic oxides was then placed in the Aminco micro reactor for treatment at 400°C under the moderate pressure of nitric acid and water vapor from the decomposition of the samples. The compositions of the products are given in Table XII. Sample CS had a composition equivalent to stainless steel waste and formed α-Fe_2O_3. Other stainless steel oxides also formed α-Fe_2O_3 in moderate amount. Sample DQ, containing iron and nickel, formed α-Fe_2O_3 and $NiFe_2O_4$. The sample CV, containing chromium, formed α-Cr_2O_3, but the intensity was much less than for α-Fe_2O_3. The 2θ values varied from 38.94° to 39.01° for the most intense α-Fe_2O_3 line for oxides from stainless steel wastes, compared with 38.81° for pure iron oxide and 39.35° for pure chromium oxide. This showed that the chromium was present as a solid

Table XI

SYNTHETIC METAL OXIDES FOR STAINLESS STEEL

Oxide	Composition of Solution[1] (molar)				Temp[2] (°C)	Analysis of Oxide	
	Fe	Cr	Ni	Other		LOI[3] (%)	X-Ray Data[4]
CS	0.75	0.17	0.08	0.14 Al	290	12.4	γ-Fe_2O_3(3)
CT	1.0				290	4.8	α-Fe_2O_3(72)
CV		1.0			290	15.2	--
DO	0.75	0.17	0.08		250	12.2	γ-Fe_2O_3(3)
DP	0.75	0.17			250	15.3	γ-Fe_2O_3(4),3.32(3)
DQ	0.75		0.08		250	12.5	α-Fe_2O_3(38)
DR		0.68	0.32		250	21.9	2.53(3)
DT	0.75	0.17	0.08	0.05 B	250	13.0	3.32(16),2.50(4),2.68(3)
DU	0.75	0.17	0.08	0.05 P	250	12.0	3.32(7)
DV	0.75	0.17	0.08	0.20 B	250	14.6	3.32(12)
DW	0.75	0.17	0.08	0.20 P	250	15.0	3.32(27),3.20(14),1.61(4)
DX	0.75	0.17	0.08		250	16.4	3.32(10),3.66(5),2.53(4)
ED	0.38	0.08	0.04	0.50 Al, 0.20 B	250	25.0	--
EE	0.38	0.08	0.04	0.50 Al, 0.20 P	250	14.5	--
EF	0.38	0.08	0.04	0.50 Al, 0.05 B	250	22.6	--
EG	0.38	0.08	0.04	0.50 Al, 0.05 P	250	19.3	--
EH	0.38	0.08	0.04	0.50 Al	250	31.2	--
ES	0.75	0.17	0.08	0.05 La, 0.05 Ce	230	23.4	3.32(9),2.53(5)
ET	0.75	0.17	0.08	0.01 F.P.[1]	230	19.0	3.32(9),2.53(5)

[1] All solutions contained 1 M HNO_3. Fe = $Fe(NO_3)_3 \cdot 9H_2O$; Cr = $Cr(NO_3)_3 \cdot 9H_2O$; Al = $Al(NO_3)_3 \cdot 9H_2O$; Ni = $Ni(NO_3)_2 \cdot 6H_2O$; B = H_3BO_3; Ce = $Ce(NO_3)_3 \cdot 6H_2O$; La = $La(NO_3)_3 \cdot 6H_2O$. For 0.01 M F.P., the molar concentrations were twice the normal concentration or $CsNO_3$ 0.0026, $ZrO(NO_3)_2$ 0.0024, $Na_2MoO_4 \cdot 2H_2O$ 0.0020, $La(NO_3)_3 \cdot 6H_2O$ 0.0012, $Ce(NO_3)_3 \cdot 6H_2O$ 0.0010, $Ba(NO_3)_2$ 0.0006, $RuCl_3$ 0.0006.

[2] Temperature for preparing oxides by heating in muffle 16 hours after evaporating solutions.

[3] LOI = Loss on ignition at 1000°C.

[4] Phases or unidentified lines are followed by intensity in divisions (enclosed in parentheses).

Table XII

STAINLESS STEEL METAL OXIDES HEATED IN MICRO REACTOR UNDER PRESSURE

Oxide[1]	Heating Conditions			Elements Present[2]	LOI[3] %	X-Ray Data[4]
	Temp (°C)	Pressure (psig)	Time (hr)			
CS	400	160	140	SS + Al	2.0	α-Fe_2O_3(42),γ-Fe_2O_3(5)
CT	400	160	140	Fe	0.2	α-Fe_2O_3(220)
CV	400	160	140	Cr	1.2	α-Cr_2O_3(20)
DO	400	335	163	SS	2.7	α-Fe_2O_3(53)
DP	400	335	163	Fe + Cr	1.2	α-Fe_2O_3(62)
DQ	400	335	163	Fe + Ni	1.0	α-Fe_2O_3(86),$NiFe_2O_4$(30)
DR	400	335	163	Cr + Ni	10.8	3.67(17),2.54(17),3.41(12), α-Cr_2O_3(6)
DT	400	400	160	SS + B	3.9	α-Fe_2O_3(46)
DU	400	400	160	SS + P	3.3	α-Fe_2O_3(51),3.30(8),3.18(4)
DV	400	400	160	SS + B	2.8	α-Fe_2O_3(32),2.54(5)
DW	400	400	160	SS + P	3.1	α-Fe_2O_3(37),3.30(33),3.18 (16),2.04(7)
DX	400	400	160	SS	5.6	α-Fe_2O_3(41)
ED	400	410	160	SS,Al,B	2.9	α-Fe_2O_3(13),5.28(11)
EE	400	410	160	SS,Al,P	3.0	α-Fe_2O_3(9),4.11(16),4.34 (10)
EF	400	410	160	SS,Al,B	3.1	α-Fe_2O_3(11)
EG	400	410	160	SS,Al,P	3.7	α-Fe_2O_3(16)
EH	400	410	160	SS,Al	3.0	α-Fe_2O_3(16)
ES	400	300	30	SS,Ce,La	5.3	α-Fe_2O_3(30),3.10(7)
ET	400	300	30	SS,F.P.	2.1	α-Fe_2O_3(53),2.92(2)

[1] See Table XI for original composition of solutions and oxides.

[2] SS = Elements in proportion for 18-8 stainless steel.

[3] LOI = Loss on ignition at 1000°C.

[4] Phases or unidentified lines are followed by intensity in divisions (enclosed in parentheses). Ignited oxides of stainless steel gave 83 divisions of α-Fe_2O_3, which is actually a solid solution of iron and chromium.

solution in the α-Fe_2O_3. (Note: In this report, the term α-Fe_2O_3 includes the solid solution of chromium and iron oxides.) The stainless steel oxides with additions of boric acid or phosphoric acid had only a slight reduction in the intensity of the X-ray line of α-Fe_2O_3, compared with samples without additives. The results indicated that boric acid and phosphoric acid might not be effective in hindering crystallization of α-Fe_2O_3.

Samples ED to EH contained aluminum as an additive to determine if aluminum would prevent crystallization due to a "zone of mutual protection against crystallization." The addition of aluminum to stainless steel (Sample ED) did not prevent the formation of crystalline iron oxide, and the reduction in intensity may have been due mainly to dilution of the iron by the alumina. Even the combination of aluminum with boric acid or phosphoric acid resulted in products with some crystalline α-Fe_2O_3.

Sample ES, with rare earths, had a lower Fe_2O_3 content than samples with boric acid or phosphoric acid as additive. Sample ET, with added fission products, was the same as previous samples without fission products.

The conclusion is that the rare earths at 0.1 molar produced the greatest reduction of crystallinity of the additives which were tested. Some reduction in crystallinity could be obtained by blending aluminum and stainless steel solutions. However, at present, the effect of crystallinity on the fluidization is not known, and it is entirely possible that solutions of stainless steel will calcine satisfactorily without additives. These studies will be helpful in interpreting the results from pilot plant studies, and in use of additives, if they appear to be desirable.

The unidentified phases in the synthetic oxides (see Table XI) were not present after heating under pressure (see Table XII) which indicates that these phases may have been basic nitrates. A variety of unidentified phases were found in the samples after heating under pressure. One phase with a d-value of 3.32 was present in samples containing boric acid, and may have contained boron. The stainless steel samples didn't contain a spinel (e.g., $NiFe_2O_4$), and the nickel could be present in an amorphous phase or an unidentified phase.

B. Fluidized Calcination of Stainless Steel Wastes

A laboratory fluidizer was operated to obtain products from fluidized calcination of acidic nitrates of stainless steel. The apparatus was the same as that described for use with aluminum nitrate. The compositions of the solutions are given in Table II, the operating conditions in Table IV, the analyses of the samples in Table IV, and the sieve analyses in Table V.

Run F8 was made with a solution of ferric nitrate, using the fluidizer with a 1.75-inch-ID Vycor tube. Solids for the bed were made by evaporating a solution of ferric nitrate to dryness and heating at 250°C. The -10 +60-mesh fraction was used. The run was operated for one day, and some caking was observed.

Run F10 was made with a solution of ferric nitrate, using the modified fluidizer with a 2.25-inch-ID tube. The run during the first two days was poor, and lumps formed in portions of the bed which couldn't be broken up easily with a Vycor rod. The product from the first two days of operation was sieved and ground to produce bed material (-20 +60-mesh) for the final day of operation. The operation during the third day was good during most of the day, with some caking occurring toward the last. The +10-mesh material consisted of a few large lumps and was separated from -10-mesh product.

Run F11 was made with a solution of stainless steel. Seven hundred ml of a solution of the same composition was evaporated to dryness and heated at 380°C. This was ground to obtain a -20 +60-mesh fraction for a starting bed material. The attrition of this bed material was very high, and some caking occurred during the first two days of operation due to inability to maintain an adequate bed in the fluidizer. The third, final, day of operation was satisfactory. Only a slight amount of caking occurred, and no large lumps were present in the product.

Run F12 was made with a stainless steel solution with boric acid added in the same manner as for run F11. Difficulty was experienced during the first two days because of an inadequate amount of bed material. The third and fourth days gave some caking due to difficulties with the nozzle. The fifth day was satisfactory.

The products from these runs were partly crystalline, whereas aluminum nitrate (run F9) gave an amorphous alumina. The intensity of the X-ray diffraction line was compared between the bed material and a similar sample ignited at 1000°C. Assuming that the intensities are proportional to the amount of crystalline oxides, then the iron oxide from run F10 was about half crystalline α-Fe_2O_3. Similarly, the stainless steel product (run F11) was about 60% α-Fe_2O_3, (Fe_2O_3 and Cr_2O_3 in solid solution). The stainless steel with added boric acid (run F12) contained about 25% α-Fe_2O_3. A minor amount of unidentified phase with a d-value at 2.94 present in a couple of samples (see Table IV). This phase was not present in the transformation studies. It was present in greater amount in the samples ignited at 1000°C and also contained X-ray lines at d-values of 4.81 and 2.40. The small amount of nickel in the stainless steel may be present in this phase.

C. Differential Thermal Analysis of Nitrates of Stainless Steel

Differential thermal analysis (DTA) was used to study the reactions which occur during the calcination of ferric nitrate and mixtures of ferric nitrate with chromium nitrate. The apparatus was the same as that used for the DTA studies on aluminum nitrate. The heating rate was 10°C per minute, and the nitrates were diluted with ferric oxide so the sample would not sink below the thermocouple when the nitrates melted. The results are given in Table XIII, and a few of the DTA curves are shown in Figure 3.

Table XIII

DIFFERENTIAL THERMAL ANALYSIS OF NITRATES OF IRON, CHROMIUM, AND NICKEL

Sample[1]	Gas	Peak Temperatures and Magnitudes[2]
FeN(25%)+Fe_2O_3 (75%)[3]	Air	64°(-4.8),S133°(-3.5),161°(-8.8),S188°(-0.8),297°(-0.8) 611°(-0.5)
CrN(25%)+Cr_2O_3 (75%)	Air	84°(-5.6),163°(-12),S182°(-5)
CrN(35%)+Fe_2O_3 (65%)[3]	Air	84°(-10.8),S118°?(-4.7),174°(-18),S196°(-7)
FeN(23%)+CrN(5%) +Fe_2O_3(72%)	Air	65°(-4.6),172°(-24),641°(-0.8),674°(-0.5)
FeN(23%)+CrN(5%) +NiN(2%)+Fe_2O_3(70%)[3]	Air	74°(-6.0),S107°(-5.9),175°(-22),656°(-0.3)
NiN(40%)+Al_2O_3(60%)	Air	68°(-8.0,163°(-7.5),232°(-6.0),331°(-6.1)
NiN(30%)+NiO(70%)[3]	Air	67°(-4.7),159°(-6.2),233°(-6.0),325°(-6.4),S340°(-2.4)
NiN(25%)+CrN(5%) +NiO(70%)[3]	Air	68°(-7.0),168°(-4.8),223°(-5.5),343°(-10.4)
NiN(15%)+CrN(20%) +Cr_2O_3(65%)	Air	60°(-1.8),83°(-5.2),187°(-18.0),568(-0.7)

[1] FeN = $Fe(NO_3)_3 \cdot 9H_2O$, CrN = $Cr(NO_3)_3 \cdot 9H_2O$, NiN = $Ni(NO_3)_3 \cdot 6H_2O$

[2] Peak temperature is followed by the differential temperature (Δt enclosed in parentheses). An "S" before the temperature denotes a shoulder on the side of a larger peak.

[3] DTA curve given in Figure 3.

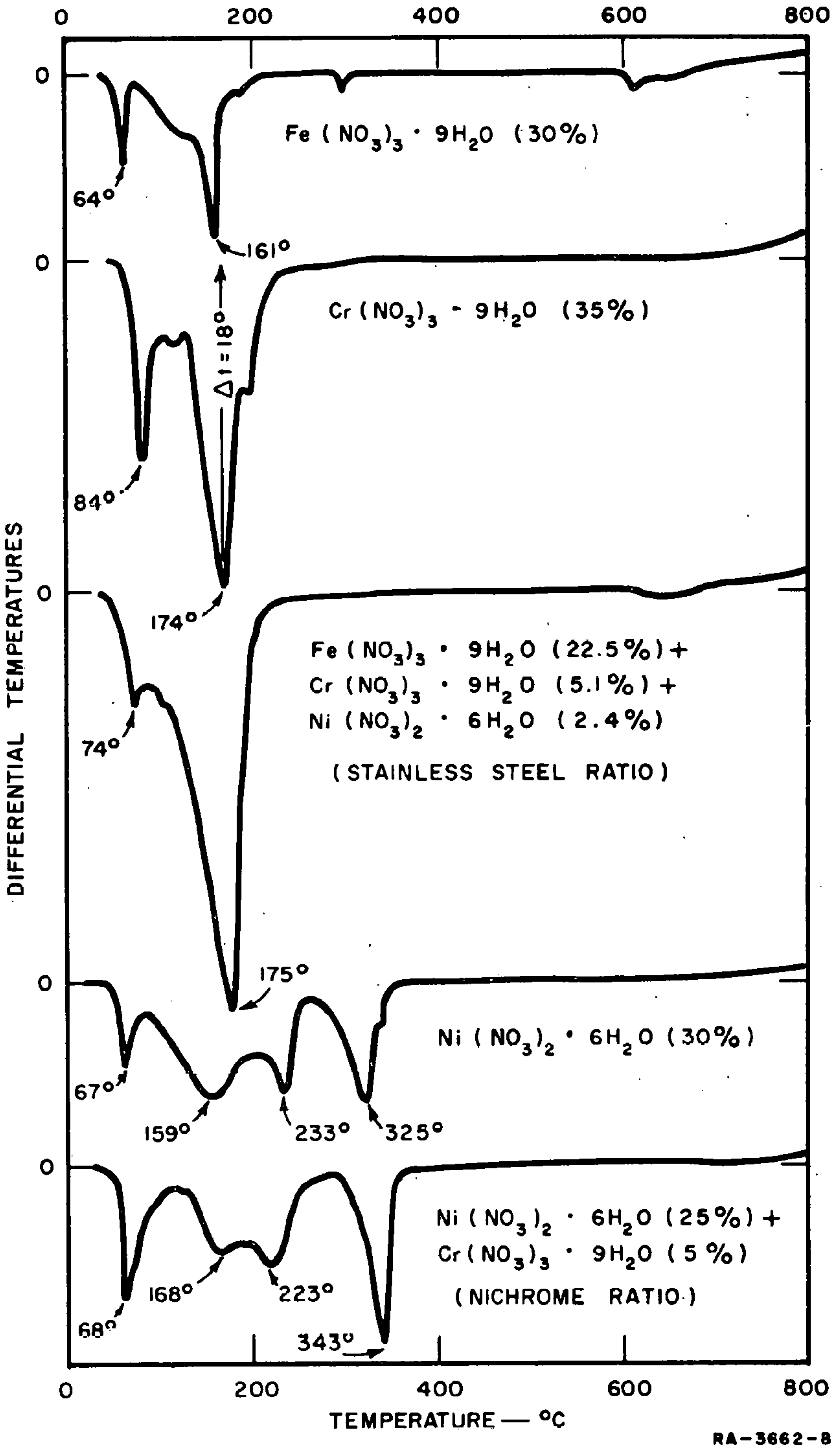

FIG. 3 DTA OF NITRATES OF IRON, CHROMIUM, AND NICKEL

Ferric nitrate diluted with ferric oxide had a peak at 64°C due to melting and a peak at 161°C due to decomposition. Chromium nitrate had a peak due to melting at 84°C, and a peak due to decomposition at 174°C.

A mixture of ferric nitrate and chromium nitrate in the ratio for stainless steel wastes had a relatively broad second peak at 172°, which is closer to that of chromium nitrate than that of ferric nitrate. A mixture of iron, chromium, and nickel nitrates in the ratio for stainless steel was about the same. The results indicate that stainless steel will be converted to the oxides at a temperature between that of ferric nitrate and chromium nitrate.

Thermogravimetric studies[2] at a heating rate of 2.6°C per minute indicated that ferric nitrate reached a constant weight at 300°C, while chromic nitrate required 500°C. A mixture of iron and chromium nitrates reached constant weight at 445°C, while iron, chromium, and nickel nitrates required 385°C. A hydrated chromic oxide or basic nitrate was reported in the range of 260 to 390°C.with chromium nitrate, but wasn't found with mixtures of chromium and other nitrates.

Karavaev[17] reported that nitric acid vapor appeared at 84°C during the decomposition of ferric nitrate and reached a maximum concentration (11.5%) at 163.5°C. With chromium nitrate, nitric acid vapor appeared at 96°C and reached a maximum concentration (4.76%) at 130°C. These results indicate that iron nitrate would decompose at a higher temperature than chromium nitrate, which is the opposite of the conclusions from the DTA and TGA results. Perhaps the heating rate caused the differences.

The conclusion from these studies is that the nitrates of stainless steel will form oxides by calcination at a lower temperature than chromium nitrate or aluminum nitrate, but not as low as ferric nitrate alone.

D. Discussion of Calcination of Stainless Steel Wastes

The laboratory studies on calcination of nitrates of stainless steel can be compared with the studies on aluminum nitrate to estimate the results on fluidized calcination of the former. The transformation studies on stainless steel, using moderate pressure, produced α-Fe_2O_3 in all cases, even with fairly large concentrations of additives (boric acid, phosphoric acid, rare earths, aluminum nitrate, and combinations). This contrasts with aluminum nitrate, which requires sodium to produce α-Al_2O_3 and produces amorphous alumina with relatively minor additions of boric acid, phosphoric acid, or magnesium nitrate.

The differential thermal analysis indicated that aluminum nitrate required a temperature greater than 300°C to complete the endothermic decomposition, while a corresponding temperature for stainless steel was 220°C. The thermogravimetric results at a heating rate of 2.6°C per minute indicated that constant weight was reached with aluminum nitrate at 440°C, while stainless steel nitrates required only 385°C. These results showed that stainless steel nitrates formed the oxides more readily than aluminum nitrate, in agreement with the easier formation of crystalline oxides from stainless steel than from aluminum.

The fluidized calcination of stainless steel wastes in the laboratory calciner produced a product with 50% α-Fe_2O_3, while aluminum wastes gave an amorphous product. The greater residence time in the pilot plant is likely to produce a completely crystallized α-Fe_2O_3. An uncertainty exists with respect to the form of the nickel in the product, but it may be present in unidentified phases or it may form a small amount of a spinel.

The fact that the operation with stainless steel nitrates was more difficult than with aluminum nitrates should not be a matter for concern at this time, because the laboratory fluidizer did not have as adequate operating controls as the pilot plant units. When pilot plant studies are made on stainless steel nitrates, the following should be considered. If the normal range of temperature produces a crystalline product which is not satisfactory as regards particle size or attrition, then trials can be made at lower temperatures (e.g., to 325°C), or with additives such as the rare earths, or both.

A study of the phase transformations in the calcination of stainless steel wastes could include a study of the many hydrates and basic nitrates of iron and stainless steel, but these have little significance because fluidized calcination gives a very rapid conversion to the oxides. The initial oxides which are formed may contain a mixture of amorphous oxides, α-Fe_2O_3 and minor amounts of unidentified phases. Further information would be desirable on the rate and factors affecting the formation of crystalline iron oxide and the form of the nickel in the product. The present studies were designed to provide an adequate background for pilot plant studies, and further studies of phase transformations will probably be required when pilot plant studies are made on stainless steel wastes.

V PHASE TRANSFORMATIONS IN CALCINATION OF NITRATES OF NICHROME

The fluidized calcination of acidic nitrates of nichrome fuels has not been studied, so the present laboratory tests were particularly needed to obtain background for future work with these wastes.

Nickel oxide, NiO, is formed by ignition of nickel nitrate, although a product containing a higher amount of oxygen can be formed by heating nickel nitrate or carbonate cautiously to about 300° in air.[18] Nickelous hydroxide is formed by precipitation and transforms to nickel oxide[19] under hydrothermal conditions at 1000 psi at 280°C. Higher nickel oxides are known, including β NiOOH and γ NiOOH.[20] Nickel oxide forms spinels (e.g., $NiFe_2O_4$) with trivalent metal oxides, such as iron, aluminum, or chromium.

Milligan and others have reported that a composition range exists for NiO-Al_2O_3 in which crystallization is hindered and which is designated as a zone of mutual protection against crystallization.[21] For example, NiO and Al_2O_3 were precipitated as a mixed gel and heat-treated at temperature levels of 300 to 700°C. In the region from 60 to 80 mole % NiO, the samples were essentially amorphous to X-rays. Studies on the NiO-Cr_2O_3-ZrO_2 system[22] showed an extensive amorphous zone of composition at 500°C, including a region at 70 mole % of NiO in the system NiO-Cr_2O_3.

A. Transformations in Nichrome Wastes

The phase transformations with nichrome (80 Ni/20 Cr.) wastes were studied in the same manner as for alumina. Synthetic oxides were prepared from acidic solutions of the nitrates, and these were heated at moderate pressure. The studies included the effect of additives such as boric acid, phosphoric acid, aluminum nitrate, rare earths, and fission products.

The compositions of the solutions are given in Table XIV. These solutions were evaporated nearly to dryness and heated in a muffle at 230 to 300°C. The compositions of the synthetic metal oxides are also given in Table XIV. At that temperature, nickel oxide was found only from nickel nitrate and in samples EI to EL, which contained aluminum nitrate in the ratio suggested for prevention of crystallization. γ-NiOOH was present in the samples prepared from stainless steel nitrates. An unidentified phase was present in the samples EU to EW, which contained a blend of stainless steel and nichrome wastes with excess nickel over the ratio to produce a spinel (e.g., $NiFe_2O_4$).

Each of the synthetic oxides was then placed in the Aminco micro reactor for treatment at 400°C under the moderate pressure of nitric acid and water vapor from the decomposition of the samples. The compositions of the products are given in Table XV.

Nickel oxide was formed in all of the samples containing a large fraction of nickel, and most of the samples also contained unidentified X-ray diffraction lines. Samples EB and EC, with boric acid and phosphoric acid as additives, had significant reductions in the amount of NiO compared with the control.

Sample EI contained aluminum and nickel in the mole ratio suggested for prevention of crystallization, but nickel oxide was formed. Addition of aluminum to nichrome, as in samples EJ to EL, gave products which contained nickel oxide.

Nickel oxide was formed in samples EU and EV, which contained a mixture of stainless steel and nichrome wastes. Sample EW, with added boric acid and added fission products, acted the same as earlier samples without added fission products.

Fission products will probably not affect the crystallinity of stainless steel or nichrome wastes. Mixing stainless steel and nichrome wastes does not appear useful to prevent formation of crystalline oxides.

Table XIV

SYNTHETIC METAL OXIDES FOR NICHROME

Oxide	Composition of Solution[1] (molar)				Temp[2] (°C)	LOI[3] (%)	Analysis of Oxides
	Fe	Cr	Ni	Other			X-Ray Data[4]
CU			1.0		290	29.5	γ-NiOOH(148),NiO(21),2.72 (28),2.47(20)
DS		0.22	0.78		250	34.1	γ-NiOOH(28),2.54(6),2.45 (6)
DY		0.18	0.82		250	37.3	γ-NiOOH(41)
DZ		0.18	0.82	0.05 B	250	50.1	γ-NiOOH(20),4.85(14), 4.37(6),2.88(6)
EA		0.18	0.82	0.05 P	250	41.3	γ-NiOOH(23)
EB		0.18	0.82	0.20 B	250	37.2	γ-NiOOH(22)
EC		0.18	0.82	0.20 P	250	38.6	γ-NiOOH(27)
EI			0.70	0.30 Al	300	27.2	NiO(54),6.8(4)
EJ		0.13	0.60	0.27 Al	300	16.5	NiO(24),2.54(6)
EK		0.13	0.60	0.27 Al, 0.10 B	300	18.8	NiO(27),3.24(4)
EL		0.13	0.60	0.27 Al, 0.10 P	300	28.6	NiO(17),2.54(7)
EM		0.02	0.08	0.90 Al, 0.14 Na	300	28.8	$NaNO_3$(27)
EU	0.38	0.18	0.45		230	42.0	4.85(11),4.37(8),2.88(7)
EV	0.38	0.18	0.45	0.01 F.P.	230	45.6	4.85(19),3.31(18),4.37(15)
EW	0.38	0.18	0.45	0.01 F.P. 0.10B	230	51.4	4.85(28), 4.37(27), 3.31(26)

[1] See Table XI for original composition of solutions and oxides

[2] Temperature for preparaing oxides by heating in muffle 16 hours after evaporating solutions.

[3] LOI = Loss on ignition at 1000°C.

[4] Phases or unidentified lines are followed by intensity in divisions (enclosed in parentheses).

Table XV

NICHROME METAL OXIDES HEATED IN MICRO REACTOR UNDER PRESSURE

Oxide[1]	Heating Conditions			Elements[2]	LOI[3]	X-Ray Data[4]
	Temp. (°C)	Pressure (psig)	Time (hr)			
CU	400	160	140	Ni	0.4	NiO(151),2.30(6),2.65(5)
DS	400	335	163	Ni+Cr	20.3	γ-NiOOH(20),NiO(28) Ni(OH)$_2$?(7),2.61(26)
DY	400	leak	67	Nic	6.0	NiO(119),2.54(15) 3.65(10),3.41(8)
DZ	400	leak	67	Nic+B	6.2	NiO(69),2.54(11),3.65(8), 3.41(7)
EA	400	leak	67	Nic+P	7.5	NiO(82),2.54(8),3.13(6)
EB	400	leak	67	Nic+B	6.9	NiO(11),2.61(10),2.48(6)
EC	400	leak	67	Nic+P	9.2	NiO(21),3.13(20),2.35(9), 4.50(8)
EI	400	320	160	Ni,Al	11.6	NiO(96),2.01(6)
EJ	400	320	160	Nic,Al	24.3	NiO(22),2.54(13),3.65(8)
EK	400	320	160	Nic,Al,B	15.4	NiO(22),2.54(15), 3.65(15)
EL	400	320	160	Nic,Al,P	19.0	NiO(22),2.54(9),3.65(6)
EM	400	320	160	Nic,Al,Na	25.4	NaNO$_3$(58),γAl$_2$O$_3$(7), 3.40(5)
EU	400	300	30	SS+Nic	6.2	NiO(19),NiFe$_2$O$_4$(18), 3.65(6)
EV	400	300	30	SS+Nic,F.P.	6.6	NiO(10),NiFe$_2$O$_4$(18), 3.65(5)
EW	400	300	30	SS+Nic,F.P.,B	6.0	NiO(13),NiFe$_2$O$_4$(20)

[1] See Table IV for original compositions of solutions and oxides.

[2] SS = Elements in proportions for stainless steel.
Nic = Elements in proportions for nichrome (80 Ni/20 Cr).

[3] LOI = Loss on ignition at 1000°C.

[4] Phases or unidentified lines are followed by intensity in divisions (enclosed in parentheses).

The unidentified phases, which were present in many of the samples, may contain the chromium. Further studies would be needed to determine the composition of these phases.

B. Fluidized Calcination of Nichrome Wastes

A laboratory fluidizer was operated to obtain products from fluidized calcination of nichrome wastes. The apparatus was the same as that described for use with aluminum nitrate. The compositions of the feed solutions are given in Table II, the operating conditions in Table III, the analyses of the samples in Table IV, and the sieve analyses of the product in Table V.

Run F13 was made with a nichrome waste, the sum of nickel plus chromium being equal to 1.5 molar. A liter of solution was evaporated to dryness and dried at 400°C to obtain material (-20 +60 mesh) for the bed. However, this material was extremely fragile and nearly all of it blew out of the fluidizer. On the third day the concentration of the nickel plus chromium in the feed solution was increased from 1.5 to 2.0 molar. The fluidizer operated poorly, with some caking and with high attrition. Operating at 400°C seemed better than at 350°C; the design of the apparatus prevented trials at higher bed temperatures. The apparatus was much more difficult to operate with nichrome than with the stainless steel or aluminum waste solutions.

Run F14 was made with nichrome waste, similarly to run F13 except that boric acid was added to the feed solution. The same difficulties were experienced as in F13: the bed material was fragile, caking occurred, and the operation was poor.

The oxides from nichrome wastes (run F13) had about 40% of crystalline NiO. With added boric acid, the ignited sample had about 40% the intensity of the sample without boric acid, and the product from the fluidizer (run F14) had about 35% of the intensity of the ignited sample. With the increased residence time in the pilot plant, compared with the laboratory calciner, the product from fluid bed calcination of nichrome wastes will probably be mainly crystalline NiO with the chromium present in a spinel, e.g., $NiCr_2O_4$, or an unidentified phase.

C. Differential Thermal Analysis of Nitrates of Nichrome

Differential thermal analysis was used to study the reactions which occur during the calcination of nichrome (80 Ni/20 Cr). The apparatus was the same as that used for the DTA studies on aluminum nitrate. The results are given in Table XIII and Figure 3 in the section on DTA of nitrates of stainless steel.

Nickel nitrate diluted with nickel oxide had four peaks at 67, 159, 233, and 325°C. The first corresponds to the melting of nickel nitrate, and the other peaks to successive steps in the decomposition of nickel nitrate.

The thermal decomposition of nickel nitrate has been reported[17] to give nitric acid vapor at 138°C, with a maximum concentration (3.22%) at 235°C. The thermogravimetric studies[2] at Idaho Falls indicated the formation of a compound at 250°C with a definite X-ray pattern and an approximate empirical formula $Ni(OH)NO_3 \cdot \frac{1}{2}H_2O$.

A mixture of nickel nitrate and chromium nitrate in the ratio for nichrome wastes had four main peaks close to those for nickel nitrate alone. However, a very marked change in the DTA occurred when the chromium nitrate was increased to an amount equivalent to the formation of spinel, and the DTA resembled that for nitrates of stainless steel. A blend of nichrome and stainless steel wastes might act similarly to stainless steel wastes in fluidized calcination.

D. Discussion of Calcination of Nichrome Wastes

The laboratory studies on calcination of nichrome wastes showed that crystalline nickel oxide was formed in transformation studies as readily as stainless steel wastes and much more readily than aluminum wastes.

The differential thermal analysis of nichrome wastes showed a peak extending to 360°C, compared with a temperature of 300°C for aluminum nitrate. The thermogravimetric data gave a temperature of 510°C for constant weight, compared with 440°C for aluminum nitrate. The data indicate that nichrome wastes require higher temperatures for forming oxides than aluminum wastes.

The fluidized calcination of nichrome wastes in the laboratory produced a product containing 40% of crystalline nickel oxide. The conclusion is that nichrome wastes will produce a crystalline product in the pilot plant, with the chromium present in an as yet unidentified phase or as a spinel.

The operation of the laboratory fluidizer was much more difficult with nichrome than with aluminum or stainless steel wastes. If the fluidized calcination of nichrome wastes was unsatisfactory but stainless steel wastes were satisfactory, then the DTA results indicate that a mixture of stainless steel and nichrome wastes in the spinel ratio would be worth trying. Possibly the operating temperature should be higher for nichrome wastes than for aluminum wastes.

A complete study of the phase transformations in the calcination of nichrome wastes would include the many hydrates and basic nitrates of nickel and nichrome. Such studies were beyond the scope of the present contract, and may be required at a later date when pilot plant studies are made.

CONTRIBUTORS

Many individuals have contributed to this project. Three who contributed generally to the over-all direction of the research and interpretation of results were Arthur G. Brown and Maurice Huggins at Stanford Research Institute and Cyril Slansky at Idaho Falls. The transformation studies were carried out by Ed Carr and Harold Eding. The chemical analyses were done by Oliver Smith, and the X-ray diffraction by Harriett Johnson. The electron diffraction studies were done by John Saunders and Don Stellman. Maurice Huggins contributed to the structural theory. Charles Lapple was consulted on cyclone design and operation.

The personnel at Idaho Falls, particularly Bob Murray and Don Rhodes, have been helpful in providing background and understanding of the problems as well as in giving suggestions.

Harold Eding

Harold Eding
Senior Physical Chemist

Maurice Huggins

Maurice Huggins
Senior Research Scientist

A G Brown

Arthur Brown
Head Physical Chemist

HE:MH:AB:tf

REFERENCES

1. Brown, B. P., E. S. Grimmett, and J. A. Buckham. Development of a Fluidized Bed Calcination Process for Aluminum Nitrate Wastes in a Two-Foot-Square Pilot Plant Calciner, Part I. Equipment Development and Initial Process Studies. USAEC Report IDO-14586. Phillips Petroleum Co., June, 1962.

2. Bower, J. R. (Ed.). Chemical Processing Technology Quarterly Progress Report, January-March, 1962. USAEC Report IDO-14589, Phillips Petroleum Co., June, 1962. Also see earlier reports in this series.

3. Eding, H. J., M. L. Huggins, and A. G. Brown. Phase Transformations in Alumina. Technical Report, May to December 1961. USAEC Report IDO-14580. Stanford Research Institute Project No. PU-3662.

4. Murray, R. F. and D. W. Rhodes. Low Temperature Polymorphic Transformations of Calcined Alumina. USAEC Report IDO-14581. Phillips Petroleum Co., September 1962.

5. Torkar, K. Investigations on Aluminum Hydroxides and Oxides. Six Parts. Monatshefte f. Chem. 91, 400-5, 450-5, 653-7, 658-68, 757-63, 764-73 (1960). See mainly pages 664, 758, and 770.

6. Newsome, J. W., et al., Alumina Properties. Technical Paper No. 10, 2nd Revision. Aluminum Co. of America, 1960, pp. 40, 50.

7. Van der Wall, E. M. Internal Letters at Idaho Falls to H. T. Hahn Van W-3-62A, July 16, 1962 and Van W-5-62A, October 17, 1962.

8. Foster, P. A., Jr. Alumina in Cryolite-Alumina Melts. J. Elect. Soc. 106, 971-5 (1959)

9. Klug, H. P. and L. E. Alexander. X-Ray Diffraction Procedures. John Wiley and Sons, Inc., New York, 1954, p. 504.

10. Stevens, J. I. (Ed.). Idaho Chemical Processing Plant, Radioactive Waste Disposal Projects, Technical Progress Report for January-March, 1960. USAEC Report IDO-14530. Phillips Petroleum Co., Sept. 9, 1960.

11. Remy, H. Treatise on Inorganic Chemistry. Elsevier Publ. Co., New York, 1956.

12. Laubengayer, A. W. and H. W. McCune. New Crystalline Phases in the System Chromium (III) Oxide-Water. J. Am. Chem. Soc., 74, 2362 (1952).

13. Maun, A. and S. Somiya. Phase Equilibrium Studies in the System Iron-Oxide-Al_2O_3-Cr_2O_3. J. Am. Ceram. Soc., 42, 603-9 (1959).

14. Milligan, W. O. and L. Merten. X-ray Diffraction Studies in the System Cr_2O_3-Fe_2O_3. J. Phys. Collid Chem., 51, 521-8 (1947).

15. Montel, G. Stability of Amorphous Coprecipitates of Fe^{III} and Al Hydroxides. Compt. rend. 250, 716-8 (1960).

16. Krause, A. and B. Niklewski, Jr. Amorphous and Crystalline Oxide Hydrates and Oxides. XXXVIII. Ber., 71B, 423-9 (1938).

17. Karavaev, M. M. and I. P. Kirillov. Thermal Decomposition of Some Nitrates. Izvest. Vyssihikh Ucheb. Zakedenii, Khim. i Khim. Tekhnol. 2, 321-7 (1959). C. A. 53, 18718h.

18. Reference 11, page 311.

19. Romo, L. A. Phase Equilibrium in the System NiO-H_2O. J. Phys. Chem., 60, 1021-2 (1956).

20. Glemser, O. and J. Einerhand. About Higher Nickel Hydroxides, Z. Anorg. u. Allgem. Chem., 261, 26-42 (1950). See also pp. 43-51.

21. Milligan, W. O. and J. T. Richardson. Magnetic Susceptibility Studies in the Dual Hydrous Oxide System NiO-Al_2O_3. J. Phys. Chem., 59, 831-3 (1955).

Appendix A

COMPOSITION OF ALUMINUM NITRATE SOLUTIONS

Solution	Composition of Solution, Molar				
	$Al(NO_3)_3$	Al[1]	HNO_3	$NaNO_3$	Other
H	1.70		1.26	1.00	
K	0.60	1.10		1.70	
BB	1.70		1.26	0.50	
BC	1.70			0.50	
BX	1.70				
BY	1.70			0.10	
BZ	1.70			0.10	0.162M H_3BO_3
CA	0.57	1.14			
CB	0.67	1.14		0.10	
CC	0.57	1.14		0.10	0.162M H_3BO_3
CD	1.70		1.26	0.10	0.85M H_3BO_3
CE	1.70		1.26	0.10	0.170M H_3BO_3
CF	1.70		1.26	0.10	0.085M H_3BO_3
CG	1.70		1.26	0.10	0.034M H_3BO_3
CH	1.70		1.26	0.10	0.085M H_3PO_4
CI	1.70		1.26	0.10	0.034M H_3BO_3 + 0.034M H_3PO_4
CJ	1.70		1.26	0.10	0.007M $Ba(NO_3)_2$ + 0.027M $CoNO_3$
CK	1.70		1.26	0.06	0.020M $Na_2MoO_4 \cdot 2H_2O$
CL	1.70		1.26	0.10	0.024M Zirconyl nitrate
CM	1.70		1.26	0.10	0.010M $Ce(NO_3)_3 \cdot 6H_2O$ + 0.014M $La(NO_3)_3 \cdot 6H_2O$
CN	1.70		1.26	0.13	1.02M H_3PO_4
CO	1.70		1.26	0.13	0.41M H_3PO_4
CP	1.70		1.26	0.13	0.206M H_3PO_4
CQ	1.70		1.26	0.13	0.041M H_3PO_4
CR	1.70		1.26	0.13	0.41M H_3BO_3
CW	1.70		1.26	0.10	0.31M $Fe(NO_3)_3 \cdot 9H_2O$, 0.06M $Cr(NO_3)_3 \cdot 9H_2O$, 0.03M $Ni(NO_3)_2 \cdot 6H_2O$
CX	1.70		1.26	0.25	0.17M H_3BO_3
CY	1.70		1.26	0.25	0.17MH_3PO_4
CZ	1.70		1.26	0.25	0.085M H_3BO_3
DA	1.70		1.26	0.25	0.085M H_3PO_4
DB	1.70		1.26	0.25	0.043M H_3BO_3
DC	1.70		1.26	0.25	0.043M H_3PO_4
DD	1.70		1.26	0.25	

Appendix A (Concluded)

Solution	Composition of Solution, Molar				
	$Al(NO_3)_3$	Al[1]	HNO_3	$NaNO_3$	Other
DE	1.70		1.26	0.25	0.085M H_3BO_3
DF	1.70		1.26	0.25	0.085M H_3PO_4
DG	1.70		1.26	0.25	0.043M H_3BO_3
DH	1.70		1.26	0.25	0.043M H_3PO_4
DI	1.70		1.26	0.25	--
DJ	1.70		1.26	0.25	0.022 H_3BO_3
DK	1.70		1.26	0.25	0.022 H_3PO_4
DL	1.70		1.26	0.25	0.011 H_3BO_3
DM	1.70		1.26	0.25	0.011 H_3PO_4
DN	1.70				0.38 H_3BO_3
EN	1.70		1.26	0.10	0.0052 F.P.[2] + 0.01 H_3BO_3
EO	1.70		1.26	0.10	0.0052 F.P.
EP	1.70		1.26	0.10	--
EQ	1.70		1.26	0.10	0.0104 F.P.
ER	1.70		1.26	0.10	0.0104 F.P. + 0.01 H_3BO_3

[1] Aluminum metal dissolved by electrolysis.

[2] Normal concentrations of fission products were taken as $CsNO_3$ 0.0013; $ZrO(NO_3)_2$ 0.0012; $Na_2MoO_4 \cdot 2H_2O$ 0.0010; $La(NO_3)_3 \cdot 6H_2O$ 0.0006; $Ce(NO_3)_3 \cdot 6H_2O$ 0.0005; $Ba(NO_3)_2$ 0.0003; $RuCl_3$ 0.0003. Total molar concentration = 0.0052.

Appendix B

COMPOSITION OF SYNTHETIC ALUMINAS

Alumina^1	Method and Temp.^{2} ($^{\circ}$C)	Alumina^3-Mole Ratios to Al_2O_3				X-Ray Data^4
		Na_2O	H_2O	NO_3^-	Other	
H	Boil-300	0.59	0.76	1.32		$NaNO_3$(143)
K	Boil-300	1.00	0.62	2.22		$NaNO_3$(81)
BB	Drip-450	0.29	0.76	0.86		$NaNO_3$(71)
BC	Drip-450	0.29	0.90	0.95		$NaNO_3$(85)
BX	Boil-200		4.72	1.97		C(150),3.87(20, 5.80(19)
BY	Boil-200	0.06	4.10	1.83		C(125),$NaNO_3$(34); 3.87(11)
BZ	Boil-200	0.06	4.38	1.98	0.10 B_2O_3	C(150),$NaNO_3$(20)
CA	Boil-200		2.31	0.89		--
CB	Boil-200	0.06	2.41	1.01		--
CC	Boil-200	0.06	2.39	1.04	0.10 B_2O_3	--
CD	Boil-300	0.06	1.51	1.04	0.46 B_2O_3	3.34(8),5.60(4)
CE	Boil-300	0.06	1.82	0.64	0.09 B_2O_3	--
CF	Boil-300	0.06	1.08	0.40	0.05 B_2O_3	--
CG	Boil-300	0.06	1.00	0.35	0.02 B_2O_3	--
CH	Boil-300	0.06	1.07	0.34	0.05 P_2O_5	
CI	Boil-290	0.06	0.90	0.38	0.02 B_2O_3, 0.02 P_2O_5	--
CJ	Boil-290	0.06	0.89	0.35	0.004 BaO, 0.009 Cs_2O	--
CK	Boil-290	0.06	0.88	0.36	0.012 MoO_3	--
CL	Boil-290	0.06	0.87	0.41	0.014 ZrO_2	3.02(5)
CM	Boil-290	0.06	1.27	0.53	0.003 Ce_2O_3 0.004 La_2O_3	--
CN	Boil-290	0.08	0.43	0.31	0.60 P_2O_5	$AlPO_4$(194)
CO	Boil-290	0.08	0.68	0.40	0.24 P_2O_5	--
CP	Boil-290	0.08	0.98	0.42	0.12 P_2O_5	--
CQ	Boil-290	0.08	0.76	0.42	0.03 P_2O_5	--
CR	Boil-290	0.08	1.05	0.61	0.24 B_2O_3	--
CW	Boil-290	0.06			S.S.^{5}	--
CX	Boil-290	0.15	0.81	0.57	0.10 B_2O_3	$NaNO_3$(11)
CY	Boil-290	0.15	0.83	0.60	0.10 P_2O_5	$NaNO_3$(11)
CZ	Boil-290	0.15	0.86	0.57	0.05 B_2O_3	$NaNO_3$(26)

Appendix B (Concluded)

Alumina[1]	Method and Temp.[2] (°C)	Alumina[3]-Mole Ratios to Al_2O_3				X-Ray Data[4]
		Na_2O	H_2O	NO_3^-	Other	
DA	Boil-290	0.15	0.88	0.57	0.05 P_2O_5	$NaNO_3$ (34)
DB	Boil-290	0.15	1.26	0.77	0.025 B_2O_3	$NaNO_3$ (38)
DC	Boil-290	0.15	1.17	0.72	0.025 P_2O_5	$NaNO_3$ (45)
DD	Boil-290	0.15	0.87	0.59		$NaNO_3$ (40)
DE	Boil-290	0.15	0.86	0.60	0.05 B_2O_3	$NaNO_3$ (27)
DF	Boil-290	0.15	1.17	0.61	0.05 P_2O_5	$NaNO_3$ (32)
DG	Boil-290	0.15	1.12	0.69	0.025 B_2O_3	$NaNO_3$ (38)
DH	Boil-290	0.15	0.92	0.55	0.025 P_2O_5	$NaNO_3$ (37)
DI	Boil-300	0.15	0.93	0.53		$NaNO_3$ (30)
DJ	Boil-300	0.15	0.97	0.61	0.013 B_2O_3	$NaNO_3$ (33)
DK	Boil-300	0.15	1.05	0.58	0.013 P_2O_5	$NaNO_3$ (30)
DL	Boil-300	0.15	1.49	0.77	0.007 B_2O_3	$NaNO_3$ (51)
DM	Boil-300	0.15	1.42	0.65	0.007 P_2O_5	$NaNO_3$ (46)
DN	Boil-300		1.72	0.64	0.22 B_2O_3	--
EN	Boil-300	0.06	1.53	0.59	0.006 B_2O_3, 0.003 F.P.[6]	$NaNO_3$ (4)
EO	Boil-300	0.06	1.57	0.65	0.003F.P.	$NaNO_3$ (1)
EP	Boil-300	0.06	1.61	0.54		$NaNO_3$ (8)
EQ	Boil-300	0.06	1.65	0.54	0.005 F.P.	$NaNO_3$ (5)
ER	Boil-300	0.06	1.86	0.60	0.006 B_2O_3, 0.005 F.P.	$NaNO_3$ (2)

[1] Aluminas prepared from solutions in Appendix A.

[2] Temperature for boil-down method is for the muffle for 16 hours. Temperature for drip method is that of the Glas-col heating mantle.

[3] Composition in moles of Na_2O to Al_2O_3, etc

[4] Alpha alumina contents are reported in percent. Other phases or unidentified lines are followed by the intensity in arbitrary scale divisions (enclosed parentheses). C = C phase, Iota = Iota Al_2O_3.

[5] S.S. = 0.182 Fe_2O_3, 0.035 Cr_2O_3, 0.032 NiO.

[6] Mole ratios to Al_2O_3 for fission products in EN and EO were RuO_2 0.004; ZrO_2 0.0004; BaO 0.0004; Ce_2O_3 0.0003; La_2O_3 0.0004; MoO_3 0.0012; Cs_2O 0.0008. Samples EQ and ER had twice this concentration.

Appendix C

ALUMINAS HEATED IN MICRO REACTOR UNDER PRESSURE

Initial Alumina[1] and Run No.	Heating Conditions			Product-Mole Ratios to Al_2O_3			X-Ray Data[3]
	Temp. (°C)	Pressure (psig)	Time (hr)	H_2O	NO_3	Others[2]	
H-633	350	230	163	1.22	1.23	Na	αH_2O(17), $NaNO_3$(270), A(20)
-649	325	200	140	0.89	1.19	Na	αH_2O(61), $NaNO_3$(230); A(6)
K-634	350	230	163	1.45	2.02	Na	α(13%), αH_2O(4), $NaNO_3$(450), A(15)
-650	325	200	140	1.06	2.05	Na	α(2%), αH_2O(43), $NaNO_3$(330)
BB-651	325	200	140	0.70	0.54	Na	αH_2O(23), $NaNO_3$(56), A(13)
BC-635	350	230	163	0.93	0.65	Na	αH_2O(19), $NaNO_3$(148), A(14)
BX-444	250	50	140	1.26	0.104		αH_2O(111)
-450	350	110	140	1.06	0.031		αH_2O(145)
BY-445	250	50	140	1.72	0.55	Na	αH_2O(36), $NaNO_3$(24)
-451	350	110	140	1.13	0.160	Na	αH_2O(154, $NaNO_3$(29)
BZ-446	250	50	140	2.12	0.77	Na, B	αH_2O(15), $NaNO_3$(18), 4.44(8)
-452	350	110	140	1.04	0.174	Na, B	αH_2O(67), $NaNO_3$(25), 5.30(16)
CA-447	250	50	140	2.71	0.90		αH_2O(6)
-453	350	110	140	1.07	0.117		αH_2O(95)
CB-448	250	50	140	4.78	1.43	Na	C(15), $NaNO_3$(13), + extra
-454	350	110	140	1.79	0.520	Na	αH_2O(34), $NaNO_3$(26), 4.76(5)
CC-449	250	50	140	5.97	2.27	Na, B	C(150), αH_2O(8), $NaNO_3$(45), + extra
-455	350	110	140	2.48	0.80	Na, B	$NaNO_3$(24), 4.81(11), 4.00(10)
CD-506	430	50	144	0.25	0.065	Na, B	$9Al_2O_3 \cdot 2B_2O_3$(160), $NaNO_3$(11)
-550	430	leak	72	0.21	0.080	Na, B	$9Al_2O_3 \cdot 2B_2O_3$(158), $NaNO_3$(14)
CE-507	430	50	144	0.27	0.054	Na, B	γ(4), A(6), AlB(4), $NaNO_3$(4)
-551	430	leak	72	0.22	0.082	Na, B	γ(4), A(5), AlB(5), $NaNO_3$(7)
CF-508	430	50	144	0.32	0.065	Na, B	γ(6), A(4), $NaNO_3$(6)
-552	430	leak	72	0.23	0.100	Na, B	γ(6), A(5), $NaNO_3$(9)
CG-509	430	50	144	0.38	0.091	Na, B	γ(6), A(4), $NaNO_3$(2)
-553	430	leak	72	0.26	0.139	Na, B	γ(5), A(7), $NaNO_3$(10)

Appendix C (Continued)

Initial Alumina[1] and Run No.	Heating Conditions			Product-Mole Ratios to Al_2O_3			X-Ray Data[3]
	Temp. (°C)	Pressure (psig)	Time (hr)	H_2O	NO_3	Others[2]	
CH-510	430	50	144	0.50	0.094	Na,P	γ(5),A(4),$NaNO_3$(5)
-554	430	leak	72	0.45	0.146	NaP	γ(4),A(3),$NaNO_3$(6),αH_2O(3)
CI-516	430	10	168	0.33	0.051	Na,B,P	γ(5),A?(2)
-533	430	305	92	0.80	0.29	Na,B,P	α(4%),A(10),$NaNO_3$(42)
CJ-517	430	10	168	0.29	0.065	Na,Ba,Cs	γ(4)
-534	430	305	92	0.48	0.234	Na,Ba,Cs	α(25%),A(14), $NaNO_3$(33)
CK-518	430	10	168	0.24	0.040	Na,Mo	γ(5)
-535	430	305	92	0.46	0.178	Na,Mo	A(21),$NaNO_3$(35)
CL-519	430	10	168	0.27	0.069	Na,Zr	γ(5)
-536	430	305	92	0.57	0.222	Na,Zr	α(5%),A(20),$NaNO_3$(36)
CM-520	430	10	168	0.36	0.104	Na,Ce,La	γ(5),3.12(9)
-537	430	305	92	0.61	0.237	Na,Ce,La	A(32),$NaNO_3$(31)
CN-527	430	370	120	0.43	0.27	Na,P	$AlPO_4$(230),$NaNO_3$(40)
CO-528	430	370	120	0.52	0.25	Na,P	$AlPO_4$(80),$NaNO_3$(38),A(4)
CP-529	430	370	120	0.63	0.26	Na,P	$AlPO_4$(22),$NaNO_3$(45),A(8)
CQ-530	430	370	120	0.58	0.28	Na,P	$AlPO_4$(3),$NaNO_3$(48),A(15)
CR-531	430	370	120	0.53	0.28	Na,B	$9Al_2O_3 \cdot 2B_2O_3$(90),$NaNO_3$(52)
CW-548	430	160	142	--	--	S.S.[4]	α(6%),αH_2O(21),$NaNO_3$(7),αFeO_3(8)
CX-662	430	130	164	0.44	0.28	Na,B	A(9),γ(6),$NaNO_3$(50)
CY-623	430	130	164	0.36	0.21	Na,P	A(6),γ(4),$NaNO_3$(33)
CZ-624	430	130	164	0.44	0.29	Na,B	A(4),γ(6),$NaNO_3$(27)
DA-625	430	130	164	0.37	0.28	Na,P	A(11),γ(4),$NaNO_3$(25),AlP(4)
DB-626	430	130	164	0.54	0.32	Na,B	A(14),γ(3),$NaNO_3$(46)
DC-627	430	130	164	1.07	0.33	Na,P	αH_2O(105),$NaNO_3$(56),AlP(9)
DD-643	430	300	290	0.44	0.35	Na	α(26%),$NaNO_3$(75),A(8)
DE-644	430	300	290	0.53	0.35	Na,B	$NaNO_3$(71),A(11)
DF-645	430	300	290	0.61	0.34	Na,P	$NaNO_3$(49),A(5)
DG-646	430	300	290	0.50	0.34	Na,B	$NaNO_3$(67),A(16)
DH-647	430	300	290	0.31	0.34	Na,P	αH_2O(21),$NaNO_3$(44),A(19)

Appendix C (Concluded)

Initial Alumina[1] and Run No.	Heating Conditions			Product-Mole Ratios to Al_2O_3			X-Ray Data[3]
	Temp. (°C)	Pressure (psig)	Time (hr)	H_2O	NO_3	Others	
DI-660	430	95	162	0.33	0.32	Na	α(36%), $NaNO_3$(47), γ(5)
DJ-661	430	95	162	0.45	0.27	Na, B	α(4%), $NaNO_3$(32), γ(4)
DK-662	430	95	162	0.48	0.28	Na, P	α(4%), $NaNO_3$(27), γ(5)
DL-663	430	95	162	0.46	0.31	Na, B	α(1%), $NaNO_3$(32), γ(5)
DM-664	430	95	162	0.54	0.32	Na, P	A(14), $NaNO_3$(36), γ(3)
DN-665	430	95	162	0.53	0.03	B	--
EN-734	430	290	160	0.28	0.13	Na, B, F.P.	α(38%), $NaNO_3$(29), A(15)
EO-735	430	290	160	0.18	0.13	Na, F.P.	α(81%), $NaNO_3$(18)
EP-736	430	290	160	0.31	0.12	Na	α(12%), $NaNO_3$(19), A(15)
EQ-737	430	290	160	0.30	0.13	Na, F.P.	α(17%), $NaNO_3$(27), A(41)
ER-738	430	290	160	0.32	0.17	Na, B, F.P.	$NaNO_3$(11), A(15)
IVA-521	430	10	168	0.77	0.16	Na	α(13%), αH_2O(9), $NaNO_3$(8)
-532	430	370	120	0.66	0.26	Na	α(29%), αH_2O(8), $NaNO_3$(37)
-538	430	305	92	0.61	0.237	Na	α(24%), αH_2O(93), $NaNO_3$(44)
-555	430	leak	72	0.89	0.20	Na	α(15%), αH_2O(45), $NaNO_3$(16)
IVA-637	350	230	163	1.02	0.19	Na	α(14%), $NaNO_3$(27), αH_2O(80)
-648	430	300	290	0.84	0.19	Na	α(18%), $NaNO_3$(10), αH_2O(45)
-653	325	200	140	1.02	0.15	Na	α(9%), $NaNO_3$(28), αH_2O(94)
22PP-626	350	230	163	0.32	0.17	Na	α(38%), $NaNO_3$(36), αH_2O(5)
-652	325	200	140				α(28%), $NaNO_3$(23), αH_2O(16)

[1] See Appendix B for original composition.

[2] Composition in moles of other elements are the same as in Appendix B.

[3] Alpha alumina contents are reported in percent. Other phases or unidentified lines are followed by the intensity in arbitrary scale divisions (enclosed in parentheses), A = A phase, γ = gamma alumina, C = C phase, $AlPO_4$ = $AlPO_4 \cdot 2H_2O$

[4] S.S. = 0.182 Fe_2O_3; 0.035 Cr_2O_3; 0.032 NiO.

Appendix D

ALUMINAS FROM IDAHO FALLS HEATED IN AIR CONTAINING HNO_3 AND H_2O

Initial Alumina[1]	Heating Conditions[2]		Product-Mole Ratios to Al_2O_3			X-Ray Data[4]
	Temp. (°C)	Time (hr)	H_2O	NO_3^-	Other[3]	
23B-P-26	500	150	0.31	0.064	Na,B	α(7%)
23B-XJP-26	500	150	0.37	0.095	Na,B	--
24-P-08	500	150	0.27	0.089	Na,B	α(11%)
24-XJP-08	500	150	0.33	0.129	Na,B	--
27P-26	500	150	0.03	0.114	Na	α(28%),γ(11),$NaNO_3$(9), 3.36(23)
27JP-26	500	150	0.10	0.219	Na	α(19%),γ(10),$NaNO_3$(28)
27-PX-28	500	150	0.048	0.130	Na	α(43),$NaNO_3$(25),Iota(35)
27-JPP-28	500	150	0.041	0.139	Na	α(5%),$NaNO_3$(51),Iota(128)
27B-P-30	500	150	0.10	0.078	Na,B	α(3%)
27B-JP-30	500	150	0.10	0.085	Na,B	--
28B-P-13	500	150	0.07	0.135	Na,B	α(1%)
28B-JP-13	500	150	0.09	0.143	Na,B	--

[1] See Table VII for original composition.

[2] Nominal composition of gas passing through the tubes was 16% HNO_3, 16% H_2O, 68% air.

[3] Compositions of other elements are the same as in Table VII

[4] Alpha alumina contents are reported in percent. Other phases or unidentified lines are followed by the intensity in arbitrary scale divisions (enclosed parentheses). C = C phase, Iota = Iota alumina, AlB = $9Al_2O_3 \cdot 2B_2O_3$, γ = gamma alumina.

PHILLIPS
PETROLEUM
COMPANY

ATOMIC ENERGY DIVISION